NAVAL POSTGRADUATE SCHOOL

MONTEREY, CALIFORNIA

THESIS

POWDER-BASED SUPERDIELECTRIC MATERIALS FOR NOVEL CAPACITOR DESIGN

by

Clayton W. Petty

June 2017

Thesis Advisor:	Jonathan Phillips
Second Reader:	Anthony Gannon

THIS PAGE INTENTIONALLY LEFT BLANK

REPORT DOCUMENTATION PAGE			*Form Approved OMB No. 0704-0188*

1. AGENCY USE ONLY	**2. REPORT DATE** June 2017	**3. REPORT TYPE AND DATES COVERED** Master's thesis

4. TITLE AND SUBTITLE POWDER-BASED SUPERDIELECTRIC MATERIALS FOR NOVEL CAPACITOR DESIGN	**5. FUNDING NUMBERS**
6. AUTHOR(S) Clayton W. Petty	
7. PERFORMING ORGANIZATION NAME(S) AND ADDRESS(ES) Naval Postgraduate School Monterey, CA 93943-5000	**8. PERFORMING ORGANIZATION REPORT NUMBER**
9. SPONSORING /MONITORING AGENCY NAME(S) AND ADDRESS(ES) N/A	**10. SPONSORING / MONITORING AGENCY REPORT NUMBER**

11. SUPPLEMENTARY NOTES The views expressed in this thesis are those of the author and do not reflect the official policy or position of the Department of Defense or the U.S. Government. IRB number ____N/A____.

12a. DISTRIBUTION / AVAILABILITY STATEMENT Approved for public release. Distribution is unlimited.	**12b. DISTRIBUTION CODE**

13. ABSTRACT (maximum 200 words)

This thesis is part of a continuing effort to improve upon the performance and fabrication methods of powder-based superdielectric material (PSDM) capacitors. This thesis reports the performance as a function of discharge time for very thin films of aqueous NaCl solution-saturated silica gel films spread within holes of a very thin (16 μm) polymer sheet. The most significant finding is that these PSDM capacitors have unprecedented, functional dielectric values for this thickness and excellent power and energy densities (≈90 J/cm^3). Earlier PSDM studies indicated that thicknesses >300 μm PSDMs have extremely high dielectric values. However, performance of these capacitors extrapolated to very thin dielectric layers was still unknown. This study recorded dielectric values of up to 1x10^9 for layers on the order of ten microns-thick. In addition, this study provides unique required engineering data regarding the performance of SDM as a function of discharge time. In summation, PSDM capacitors were successfully tested as a function of frequency and form factor for various thicknesses.

14. SUBJECT TERMS capacitor, material science	**15. NUMBER OF PAGES** 77
	16. PRICE CODE

17. SECURITY CLASSIFICATION OF REPORT	**18. SECURITY CLASSIFICATION OF THIS PAGE**	**19. SECURITY CLASSIFICATION OF ABSTRACT**	**20. LIMITATION OF ABSTRACT**
Unclassified	Unclassified	Unclassified	UU

NSN 7540-01-280-5500 Standard Form 298 (Rev. 2-89)
Prescribed by ANSI Std. 239-18

THIS PAGE INTENTIONALLY LEFT BLANK

Approved for public release. Distribution is unlimited.

POWDER-BASED SUPERDIELECTRIC MATERIALS FOR NOVEL CAPACITOR DESIGN

Clayton W. Petty
Lieutenant, Junior Grade, United States Navy
B.S., United States Naval Academy, 2015

Submitted in partial fulfillment of the
requirements for the degree of

MASTER OF SCIENCE IN MECHANICAL ENGINEERING

from the

NAVAL POSTGRADUATE SCHOOL
June 2017

Approved by: Jonathan Phillips
Thesis Advisor

Anthony Gannon
Second Reader

Garth Hobson
Chair, Department of Mechanical and Aerospace Engineering

THIS PAGE INTENTIONALLY LEFT BLANK

ABSTRACT

This thesis is part of a continuing effort to improve upon the performance and fabrication methods of powder-based superdielectric material (PSDM) capacitors. This thesis reports the performance as a function of discharge time for very thin films of aqueous NaCl solution-saturated silica gel films spread within holes of a very thin (16 μm) polymer sheet. The most significant finding is that these PSDM capacitors have unprecedented, functional dielectric values for this thickness and excellent power and energy densities (≈90 J/cm^3). Earlier PSDM studies indicated that thicknesses >300 μm PSDMs have extremely high dielectric values. However, performance of these capacitors extrapolated to very thin dielectric layers was still unknown. This study recorded dielectric values of up to 1x10^9 for layers on the order of ten microns-thick. In addition, this study provides unique required engineering data regarding the performance of SDM as a function of discharge time. In summation, PSDM capacitors were successfully tested as a function of frequency and form factor for various thicknesses.

THIS PAGE INTENTIONALLY LEFT BLANK

TABLE OF CONTENTS

LIST OF FIGURES

LIST OF TABLES

THIS PAGE INTENTIONALLY LEFT BLANK

LIST OF ACRONYMS AND ABBREVIATIONS

C	capacitance
d	distance
DEW	directed-energy weapons
DI	deionized water
EDLC	electric double-layer capacitors
ED	energy density
ε	dielectric constant (Epsilon)
F	farad
Hz	hertz
IS	Impedance Spectroscopy
J	joules
J/cm^3	joules per cubic centimeter
m	meters
m^3	cubic meters
mA	milliampere
MW	megawatt
NaCl	sodium chloride
NPS	Naval Postgraduate School
PEA	Percent Effective Area
PD	Power Density
PSDM	Powder-based Superdielectric Material
SDM	Superdielectric Material
t	time
TSDM	Tube-Superdielectric Material
USN	United States Navy
V	volts
W	watts
W/cm^3	watts per cubic centimeter

THIS PAGE INTENTIONALLY LEFT BLANK

ACKNOWLEDGMENTS

I would like to thank my advisor, Professor Jonathan Phillips, for his support and encouragement throughout my time at the Naval Postgraduate School. Specifically, thank you for teaching me to buck the status quo and that it's never too late to think outside the box. I would also like to thank Professor Claudia Luhrs for reaffirming in me that maintaining an unwavering pursuit of knowledge is to lead a life worth living. Additionally, I must express my extreme gratitude to ENS Mitch Heaton, whose help with data analysis was invaluable.

I would also like to thank my family and friends whose love and support have propelled me to discover new heights during my time in Monterey; I will remain forever grateful.

THIS PAGE INTENTIONALLY LEFT BLANK

I. INTRODUCTION

A. SUMMARY OF FINDINGS

This thesis was designed to test a simple hypothesis: previously studied power-based superdielectric materials (PSDM)s shown to have dielectric constants on the order of $1x10^{10}$ can be used in very thin layers to produce capacitors with unprecedented energy and power densities. More specifically, thin perforated sheets of plastic could give structure to a gel-like dielectric material comprised of aqueous salt solution and fumed silica to produce an overall energy-dense capacitor. The findings presented herein support this hypothesis. In fact, on a volumetric basis, these thin PSDM capacitors are three times better than commercial supercapacitors at long discharges and mark a significant step forward in high-energy density capacitor research [1].

B. MOTIVATION AND BACKGROUND

Modern weapons technologies require more and more power, and with it a need to store this energy in reserve. New directed energy weapons (DEW) like the Laser Weapon System (LAWS) or the rail gun not only require vast amounts of stored energy, but also require this energy be delivered extremely quickly as electrical energy [2]. Power is the rate at which this energy is delivered given in Equation (1):

$$Power = \frac{Delivered\ Energy}{Time}\ [=]\ J/s\ [=]\ W \tag{1}$$

However, the best means available to deliver this electrical power are current generation supercapacitors which require a volume too large to accommodate on Navy ships or other expeditionary warfare outposts. Consequently, to enable practical deployment, the military is looking for a new generation of capacitors that are both energy and power dense. These capacitors cannot be hindered by size, weight or operating cost constraints that fielding-prohibitive [3].

It is widely accepted that current state-of-the-art batteries such as lithium ion found in cars, smartphones and other devices have adequate energy densities but lack optimal electric power delivery performance [4]. Stated differently, their characteristics

to date suggest these batteries can store many Joules of energy within a certain volume, but they are often unable to discharge at fast rates (i.e., deliver high current). Such limitations are often chemical in nature. Batteries store energy due to differential chemical potentials; they are inherently limited as to the rate of chemical reaction, and over-exerting them on discharges can be hazardous as well as cause physical damage to the electrodes [5].

Conversely, capacitors store energy electrostatically by releasing excited state electrons collected on a conductive electrode, providing immediate and efficient power [6]. These power, energy, and time tradeoffs exist between batteries and capacitors. Batteries clearly lead capacitors in energy density. In particular, rechargeable Li-ion batteries are clearly the best variety. However, no battery type delivers power over short time frames that effectively competes with capacitors highlighted in Figure 1. In turn, this mode of energy storage makes capacitors ideal for high power applications as discharging is theoretically nearly instantaneous, and it is not encumbered by ionic transport as is the case in batteries [5]. Yet, current capacitors are significantly less energy dense than modern-day batteries [7]. Indeed, many power systems are designed to use these two types of energy storage synergistically, as in the case of hybrid energy storage modules (HESMs) where batteries carry the typical normalized daily loads and capacitors serve to meet peak demands that are shorter in duration [3].

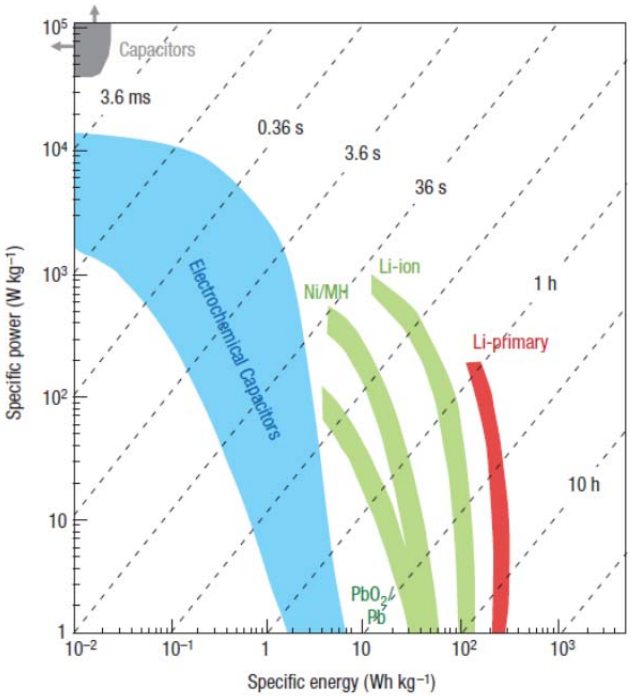

Figure 1. Specific Power vs. Specific Energy of Electric Storage Device. Source: [8].

Thus, there still exists a need for high energy density, high power density storage solutions. As seen in Figure 1, batteries may have high specific energies but do not satisfy the power requirements for which capacitors currently present an alternative. However, one of the greatest challenges faced by modern capacitors is size. The capacitor bank needed to fire a new weapon like the electromagnetic railgun would take up a volume of roughly 31.0 m^3, according to Lombardo using values from Stewart [9], [10]. Space on that order of magnitude simply does not exist on the proposed platforms for these weapons systems, like the DDG 1000 Zumwalt-class destroyer.

Ideal capacitors would rival the energy density of the best batteries, require smaller volumes, and present far superior power densities. Lithium-ion batteries average 200J/cm^3 [11], the newest of which have a volumetric energy density between 900 to 2230 J/cm^3 (250 to 620 Wh/L) [12]. According to Lombardo [10], if current capacitors could meet the 1000 J/cm^3 threshold [13], the volume of the capacitors required to launch

railgun projectiles would be reduced by a factor of 30. The best commercially available electric double layer capacitors (EDLC), or "supercapacitors," are known to be the best for energy storage ($35J/cm^3$) [1]. Thus, the current state-of-the-art supercapacitors achieve approximately a tenth of the energy density of the best lithium ion batteries.

A fundamental shift in capacitor technology is imperative if we expect to use these novel weapons systems in practice. Furthermore, the emergence of "Internet of Things (IoT)" technologies continue to drive demand for independent, portable energy storage applications. To meet this challenge, a new class of supercapacitors must fill this void. The Materials Science capacitor working group at the Naval Postgraduate School (NPS) invented a new class of dielectrics known as "superdielectric materials" (SDMs) and come in several different forms including Tube SDM (TSDM), Fabric (FSDM), and Powder (PSDM). Capacitors made with these dielectric materials exhibit extremely high dielectric values which, in turn, result in promising energy and power density characteristics [14].

This thesis focused on the powder form of SDMs, the powder kind. However, prior work studied thicker layers of SDMs [15]. The aim of this thesis is to find a simple method to create thin PSDM capacitors and test the "projected thick-layer" energy densities based on thick-layer studies against real experimental data. Also, this thesis is the first study of the behavior of PSDM as a function of discharge time. Indeed, novel Navy weapons will operate with discharge times on the order of 0.005s [16]; hence, capacitors must be tested (certified) for power density at this time scale as well. Thus, detailed characterization of capacitor performance as a function of discharge time is necessary for the robust engineering designs of future Navy power systems.

C. RESEARCH OBJECTIVES

The main objectives for this thesis research are threefold and each center on three new PSDM design parameters. First, the PSDM layers must achieve micron-size thicknesses. In order to ensure this, an additional nonconducting material in the form of thin polymer sheets of known thickness was used as an insert of sorts; to the insert was to be perforated to allow for the PSDM to fill those voids. This moreover contributed to the

second objective of using stable, inexpensive materials to provide for mechanically robust macroscopic construction appropriate for large scale production. The last objective of this research was to develop this thin PSDM capacitor design that would still allow for very large dipoles to act within the dielectric—the crux of the current SDM model—and, by extension, yield even better overall performance.

What follows are the successful findings of this research, which met all objectives, and yielded new insights into these novel form factors that point to further avenues for exploration.

D. CAPACITOR THEORY AND GOVERNING EQUATIONS

A general overview of capacitor theory is presented as a means of highlighting key physics principles applicable to this research. First, the concept of capacitance, or a body's ability to store an electrical charge, is covered. Capacitance is defined as the amount of charge an object can hold at a given voltage and is presented in Equation (2)

$$C = \frac{Q}{V} = \frac{\text{Charge}}{\text{Potential Difference}} \tag{2}$$

where Q is the charge given to one plate and V is the potential difference of volts [17].

Several different constructions of capacitors exist. The simplest and form used in this research is parallel plate capacitor construction. In this arrangement, electrostatic energy is stored in the form of electrons in a capacitor when a voltage is applied to an insulating medium separated by two conducting surfaces [18]. Electrons are collected on one of these conducting surfaces, and an induced electric field is created between the plates (see Figure 2).

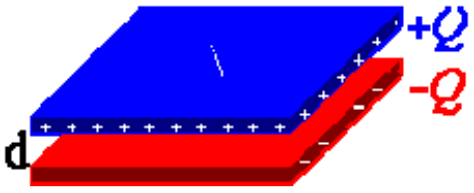

Figure 2. Parallel Plate Capacitor. Source: [19].

Often, a dielectric material (something other than air) is put between these plates as a means of counteracting the induced field, thereby enabling more charge *Q* to be stored per unit of voltage *V*. Consequently, this would have the effect of increasing the capacitance *C* as per Equation 1. Additionally, *C* can also be described by Equation 3

$$C = \frac{\varepsilon \varepsilon_o A}{t} \tag{3}$$

where *A* is the electrode area, *t* is the thickness of the dielectric (also seen in Figure 2 as *d*, distance between the plates, ε is the dielectric constant of the material, and ε_o is the permittivity of air, 8.85E-12 [farads per meter].

Based on Equation 3, there are three factors that can be used to improve capacitance; cross sectional area, dielectric thickness, and dielectric constant. The vast majority of research on high power delivery capacitors is on EDLC supercapacitors. This research effort centers on increasing the surface area of the electrodes *A*. This is done by replacing the very low surface area metal electrodes with high surface area material, generally some powder form of highly conductive carbon.

A Ragone plot is a means of depicting energy and/or power densities and generally outlines areas where current and future technologies lie as compared to one another. Figure 3 illustrates where current supercapacitor and battery technologies exist as well as highlights the desired goal of all energy storage solutions [20].

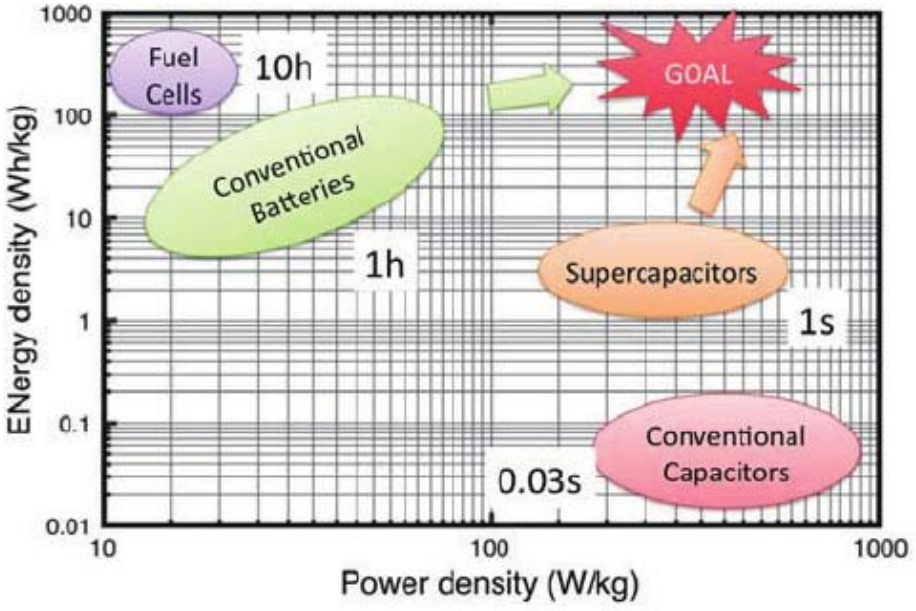

Figure 3. Ragone Chart of Existing Commercial Energy Storage Technologies. Source: [20].

Previous thesis work at NPS by Gandy [21], Fromille [14], and Cortes [22] has proven that another method of improving capacitor performance exists as per Equation 3. By improving the dielectric constant as opposed to increasing the surface area, the NPS capacitor group has demonstrated unprecedented dielectric constants. These materials are known as superdielectric materials (SDMs), and the physics principles to which they adhere are covered in the next section. Previous to this work, $BaTiO_3$ was the material with the largest known dielectric constant, on the order of 10^4. Fromille and Phillips [13] demonstrated porous alumina, sufficiently filled with NaCl dissolved in water to create "paste"-like material, consistently had dielectric constants on the order of 10^9.

However, energy density—and by extension, power density—is the true metric to convey improved capacitor performance. A capacitor's energy density is given by the following relationship

$$Energy\ Density = \frac{\frac{1}{2}(C\,V^2)}{\text{Capacitor Volume}} = \frac{\frac{1}{2}\frac{\varepsilon\,\varepsilon_o\,A}{t}V^2}{(A\cdot t)} \equiv \frac{\varepsilon\,\varepsilon_o\,V^2}{2t^2} \tag{4}$$

where V is the max charge voltage and t is the thickness of the dielectric (distance between the plates as in Equation 3).

Higher energy density requires both increasing the dielectric constant and minimizing the distance between plates. The powder based dielectrics developed in the early SDM studies proved to be difficult to use in very thin dielectric layers [15]. Thus despite impressive dielectric values, the distance (t) between electrodes was too large and the resultant energy densities were not ideal. Moreover, other work suggests simple extrapolation of dielectric values to thin layers can be misleading. Factors scale as "saturation" and "breakdown" effects can make extrapolation unreliable.

The aims of this thesis, however, were to create very thin layers to directly determine if dielectric values for PSDM can in fact be extrapolated and to directly measure energy densities of these capacitors. By using an electrically non-conductive matrix wetted by an electrolyte solution saturated with dissolved ions, very high dielectric constants were again attained and in this case, for the first time, micron-scale thicknesses were achieved. The consequence was higher energy and power densities as previously only postulated.

E. SDM MODEL

The concept of a superdielectric material stems from the generally accepted theory on dielectrics which states that these materials exist to counteract the induced field between the plates of a parallel plate capacitor. If the size of these induced electrostatic dipoles can be maximized, they will more effectively cancel the dipole field from the electrodes. Ferroelectrics, such as barium titanate ($BaTiO_3$), were known to be the best solid dielectrics which form the largest dipoles of all solids when polarized by an electric field. In fact, this is found to be true for solid dielectrics, even though the "length" of the dipoles formed in barium titanate, via a separation of (Ba^+) and (O^-) ions, are estimated to be no longer than 0.1 Å [23].

Per this dielectric theory, the first SDM dielectrics were designed to have very long dipoles. Specifically, it was theorized that in aqueous solutions containing dissolved

salt solutes, cations and anions will move in orientations opposite an applied field. This in turn creates dipoles equal in length to the average ionic separation. The length of the polarized "unit of water" and the ion concentration created from the dissolved salts determine the dipole concentration. A general depiction is shown in Figure 4.

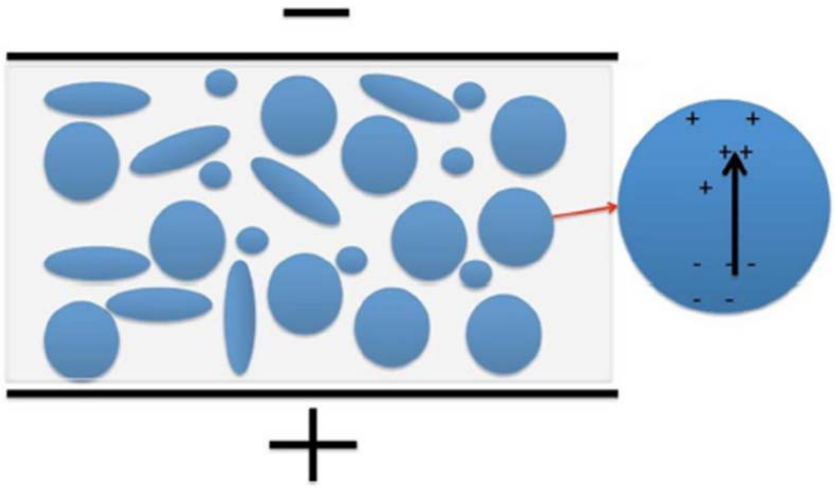

Figure 4. Dipole Formation in a Powder Superdielectric Material. Source [23]

In Figure 4, the dielectric between the two electrodes can be modelled as water drops (blue) containing dissolved salt filling the pores of a non-electrically conductive matrix media. Each individual drop (right side) can be modelled as a "unit of water" containing a definitive concentration of ions. The ions migrate toward the electrode of opposite charge. In the illustrated case the cations migrate toward the negative electrode and the anions toward the positive electrode.

The specific material employed as the first invented/discovered SDM was a high porosity powder, a form of alumina, filled with a solution of deionized (DI) water saturated with boric acid. In practice, this creates a material with the mechanical consistency of slightly wet paste. This form of SDM is now called PSDM [13].

In water, boric acid dissolves to create (+) ions and (-) ions. In the field created between the two electrodes of a parallel plate capacitor the (+) ions will move toward the

negative electrode and the (-) ions toward the positive electrode. This will create a long electric dipole [13].

There are several empirical aspects of the behavior of SDM that imply limitations to the use of SDM based capacitors for high energy density storage and power delivery. In the first study, it was found there was an ultimate limit to the voltage of ~1.4 volts [13]. It was argued that above this voltage there is a breakdown ("electrolysis") of water that creates a short circuit. Similar phenomena are believed to limit the ultimate voltage of aqueous based supercapacitors [23]. Second, above 0.8 volts there is a sharp drop in capacitance. Again, a similar phenomenon is observed for supercapacitors, although, the creation of different regions of capacitance is not always observed until higher frequencies. Third, the dielectric constant of the original PSDM material was found to be intrinsic to the material. That is, the measured net capacitance was inversely related to the dielectric layer thickness over a wide range of thicknesses, as related in Equation 3. Finally, all capacitance values were based on the R-C time constant measurement method, and the discharge times were from hundreds to thousands of seconds [24]. Later studies established that the dielectric constant values "roll-off" with frequency, suggesting the recorded dielectric values from this first study are in fact upper limits.

The results of the second study of PSDM were consistent with the general SDM theory that any solution containing dissolved ions in a liquid phase will act as an SDM [14]. The second study employed the same alumina as the first, but used three different concentrations of NaCl (salt) solution to contain the ions in a liquid phase. An outcome of the second study was to test a model quantitatively. Dipole strength is a linear function of two parameters: dipole length and the charge of the dipole. In this first quantitative model of SDM behavior, it was assumed that the relative dielectric constant of two materials is simply the ratio of the net dipole strength [23].

$$Dielectric\ Constant\ Ratio = \frac{Dipole\ Length_{\ 1} \times Mobile\ Charge\ Density_1}{Dipole\ Length_2 \times Mobile\ Charge\ Density_2} \quad (4)$$

This equation was employed to predict the dielectric constant ratio between the aqueous salt solution SDM (Material 1) and barium titanate (Material 2) with a presumed dielectric constant of 1,000. The mobile charge density of a solid, for example $BaTiO_3$, is

equal the density of the ions within the solid which "move" to form dipoles [23]. The simple model did not fit the data. Specifically, the model suggested the dielectric constant of the first PSDM would be one-thousand times higher than barium titanate. In practice dielectric constants one million times higher than $BaTiO_3$ were measured.

It was also found that the salt and the "matrix" material impact the ultimate dielectric constant. Indeed, PSDMs with dielectric constants as high as 60 billion (6.0×10^{10}) were created in PSDM consisting of aqueous sodium chloride solutions (salt water) in the same alumina used in the first study.

In a third study of PSDM the effect of matrix material selection was studied. Fumed silica was used instead of porous alumina. The measured dielectric constants for very slow discharges were about a factor of two higher than those observed below 1.0 volts using the alumina material, approximately 1.1×10^{11}. These measurements were recorded for capacitors with distance between plates of just over 2 mm and at high concentrations of NaCl (approx. 30 wt%) dissolved in DI water [15]. Given an average particle size in fumed silica of ~5 nm and subsequent anticipated value of the dielectric constant as per Equation 4, questions of dipole size were raised. Indeed, the pore dimensions for packed particles should be of the order of the particle size. According to theory, a "pore" with a dimension of 5 nm filled with "salt water" will not display significant SDM like behavior. However; it is well known that the particles in wet fumed silica do not simply arranged in a random fashion but rather via ordered hydrogen bonding allowing pore networks to form [23]. The effective pore length in this case is difficult to model accurately. To a first order approximation it was assumed the diffusion length equals the total distance between electrodes.

In order to explore this first-order model, the impact of total dielectric thickness on the dielectric constant was studied and it was found, unlike the case for the alumina based SDM, that the dielectric constant decreased steadily with decreasing distance between electrodes. This was interpreted to be consistent with the model for fumed silica based SDM: the effective pore length is proportional to the distance between the electrodes [23]. Importantly, thin PSDM form factors were explored in this research in

direct contradiction to the extrapolation of this first-order model to evaluate the compromise in dielectric performance versus reducing the thickness as a means of increasing capacitance directly.

Another avenue of study initiated in this third PSDM study was the impact of frequency on the effective capacitance of SDM. For frequency dependence measurements, the charging/discharging protocol was also changed from "RC time constant" to "constant current" using a commercial galvanostat (BioLogic VSP-300). This study was undertaken because the theory of SDM suggests a relatively slow development of dipoles and concomitantly high dielectric values. Indeed, SDM are based on field driven convection of ions inside the liquid filling the pores of the electrically insulating matrix material. Given sufficient time this leads to the creation of "giant" dipoles [23].

Phillips, Quintero, and Suarez assert that there is a time dependence for ionic motion to form multi-micron length dipoles [23]:

> Ions initially randomly dispersed in a liquid must travel the order of the thickness of the dielectric layer to become more ordered and form giant dipoles, as seen in Figure 5… This model of multi-micron ionic travel under the influence of an applied field implies a time dependence to the capacitance of SDM. Qualitatively, the model clearly indicates that if the applied field is switched too quickly from one polarity to the opposite, the net ionic separation will be reduced. The ions that form the dipole will simply not have time to travel to their equilibrium, fully polarized, positions. This in turn implies smaller effective dipoles at higher frequency. This should lead to a smaller measured dielectric and capacitance values with increasing frequency.

This would imply, to a degree, that dielectric materials may be chosen to optimize their power and energy density properties. More testing is required to fully validate this hypothesis.

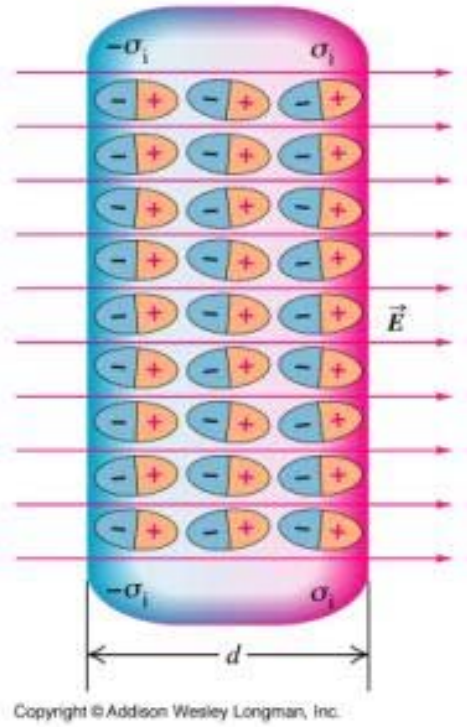

Figure 5. Polarization of Dielectric Material. Source: [25].

It was clearly shown that the dielectric constant and capacitance decreased as the discharge period decreased [10]. It was roughly found that the dielectric constant for a discharge time of 1 second was an order of magnitude less than that measured for a discharge time of ten seconds. However, a true general rule was not found as other factors such as dielectric thickness and salt concentration were found to impact the rate of capacitive "roll off" with decreasing discharge time. To summarize, the study did suggest that for SDM the roll off of capacitance is significant even for relatively "long" (e.g., 1 second) discharge times; although the net "power" delivered actually increased with decreasing discharge time. This reflected the fact that during the discharge at higher frequency less energy is released, as per a decreased capacitance, but it is released more quickly [23].

The success of the SDM theory as applied to PSDM suggested that matrix structures other than packed particles might work as well. In particular, the dielectric properties of Tube-Superdielectric Materials (TSDM) (anodized titania films) filled with

various aqueous salt solutions were studied. As shown in Figure 6 upon anodization an oxide film consisting of connected "pillars" of TiO_2, orthogonal to the original surface, form.

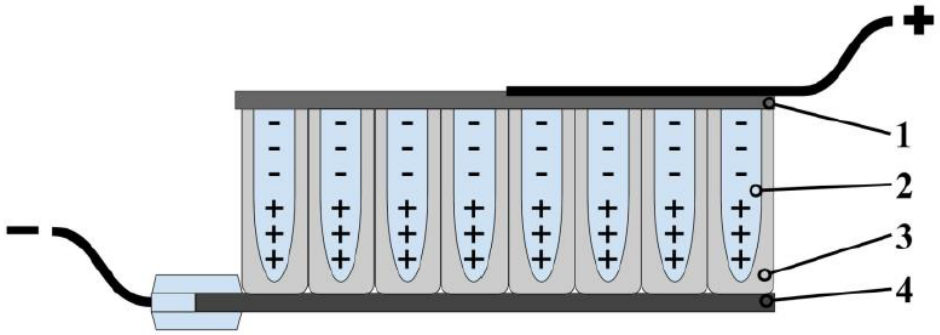

Grafoil positive electrode (1), aqueous electrolyte (2), tubular oxide structure (3), and metal substrate as negative electrode (4).

Figure 6. Schematic of TSDM Capacitor. Source: [21].

Between the pillars a regular array of open pores, generally of the order 100 nm across and as deep as the oxide film, are found. According to the SDM theory, once filled with an aqueous salt solution these structures should be excellent dielectrics, as large dipoles of the same length–generally many microns–as the pores should form.

As anticipated, the dielectric constants for these materials were extremely high, but a function of the pore length [21]. In the first study aqueous sodium carbonate solutions were used to fill the pores of anodized titania of various lengths. Even for pores as short as ~3 micron the dielectric constant was greater than 10^7 for long discharge times (approximately 100 seconds) even at 2 volts. The thicker the oxide layer, the larger the dielectric constant. For 18 micron pores the dielectric constant was consistently $>10^8$, again even at 2 volts [21].

Due to the promising nature of these early SDM results and once a greater understanding of the greater SDM model was known, new areas to improve these capacitors became clear. Specifically, this thesis sought to explore fabrication processes

for PSDM capacitors that enabled very small thicknesses, thereby reducing *t* in Equations 3 and 4 and improving the overall energy and power density characteristics of the next generation PSDM capacitors.

F. MEASUREMENT METHODOLOGIES

1. Capacitor Performance Measurements Overview

It should be noted that reports in capacitive performance vary not only in the metrics reported, but also in the techniques used to measure them. For proper circuit design the relevant parameters include some, or all, of the following: capacitance, capacitance as a function of frequency, energy density, energy density as a function of frequency, dielectric value, dielectric value as a function of frequency, equivalent circuit parameters for internal resistance and output resistance, power output, power output as a function of discharge time, and safe operational voltage range. Through the efforts of the Materials Science Working Group, the metrics that are most informative for actual engineering implementation in the Navy's context have been emphasized: namely, capacitance, dielectric constant, energy density, and power density.

There are four major approaches to measuring capacitance that are presently in use: RC time constant, impedance spectroscopy (IS), cyclic voltammetry based on controlled linear increase/decrease in voltage with time, and constant current employing a galvanostat. There are advantages and disadvantages to each of these methods, namely in the types of data on which each can more accurately report. For the purposes of this thesis research, the constant current method was chosen as most appropriate for the data desired to be collected and most accurate.

2. Constant Current Method

One of the primary methods used in capacitance measurements is the constant current method, generally conducted using a programmable galvanostat. The basis of the method is derived from taking the derivative of Equation 5, and the assumption that capacitance is a constant value at all voltages. More generally [23],

$$\frac{d(C)}{dt} = \frac{d(\frac{q}{V})}{dt} = 0 \tag{5}$$

This reduces to:

$$\frac{-q}{V^2}\frac{dV}{dt} + \frac{1}{V}\frac{dq}{dt} = 0 \tag{6}$$

and in the constant current ($\frac{dq}{dt} = I$) case this reduces to:

$$\frac{I}{\frac{dV}{dt}} = C \tag{7}$$

The method reveals interesting behaviors for both EDLC and SDM capacitors. There is a clear non-linear response from both of these types of capacitors, even at low frequencies. This is consistent with existing observations that these supercapacitors are unsuitable for any type of high frequency electronics. Outside power supplies, supercapacitors will not be found in computers, cell phones, radios, etc. as a standalone energy storage method. General charge and discharge cycling is shown in Figure 7.

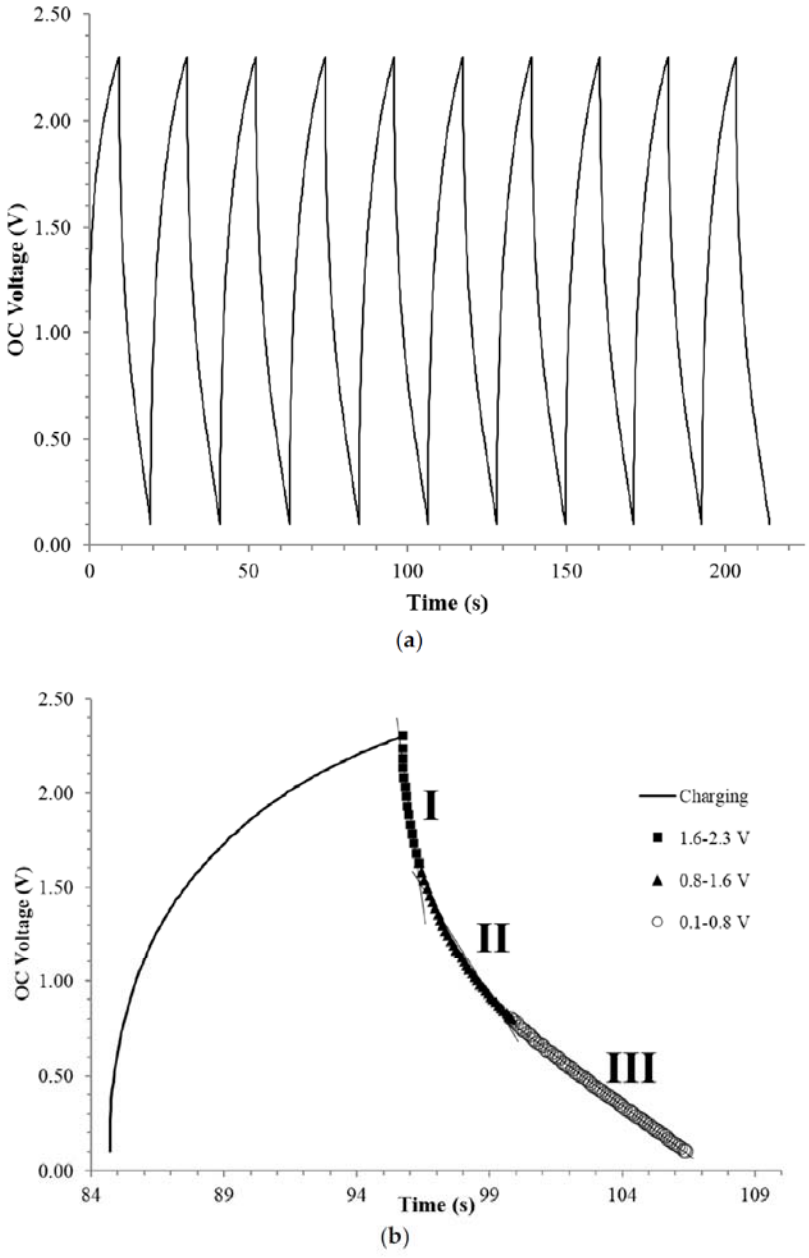

Figure 7. Structure of Discharge. Source: [24]

Example of raw, constant current data for a PSDM capacitor is shown in Figure 7. On top in (a), there are ten cycles, with an average discharge time of ~9s. In (b), upon closer inspection of a discharge, there appear to be three distinct regions of characteristic capacitance as defined over different voltage regions (I, II, and III). With the exception of Region III, discharge rates are shown to be extremely non-linear. Thus, this behavior suggests capacitance is a function not only of voltage, but also of frequency. However, capacitance is generally observed to be nearly constant over voltage ranges <1 volt [23].

The tool used to measure capacitance has a major impact on the reported results. Constant current analysis provides reliable information regarding energy and power characteristics over a broad range of frequencies, but cannot provide single metric values as a function of frequency. Therefore, many trials are conducted in order to aggregate results which lead to frequency extrapolation based on varying average discharge times.

3. FHS Method

Recent commercial EDCL testing has also pursued a technique that may further enhance the observed performance of the tested capacitors. Annotated in one of their technical notes, the company Murata implements a technique whereby they charge a capacitor to a rated voltage, hold the voltage with a varying current and then discharge the capacitor to a set voltage [26]. The Murata technique, renamed Fast-Hold-Slow (FHS), was also used and applied to this research with PSDM capacitors. Principally, this method would seem to allow the dipoles within the SDM matrix extra time to align and lengthen during the charging phase more fully, thereby maximizing their effective dielectric properties. Ultimately, this will in turn result in measuring the highest energy density possible for a given electrolytic solution.

4. Key Assumptions

Key assumptions throughout experimentation involved environmental conditions including temperature, pressure and relative humidity. Every effort was made to keep these external factors consistent. Namely, room temperature and was kept relatively consistent at around 25 °C. Furthermore, these aqueous-based electrolyte solutions will

eventually evaporate when exposed to the normal atmosphere. Thus, a crude humidity control was put in place over the capacitor testing apparatus to keep the relatively humidity higher such that the electrolyte would not dry out during testing. Greater detail is given in the chapter.

THIS PAGE INTENTIONALLY LEFT BLANK

II. EXPERIMENTAL METHODS

A. OVERVIEW

Five novel capacitor designs were created to test a new family of PSDM capacitors: ones where a thin polymer sheet was inserted between the electrodes of very small thickness to add structure to the PSDM gel. Holes were cut and filled with the "Superdielectric Material." In this thesis research, the SDM implemented was fumed silica saturated with a 30 wt% NaCl salt solution; the result was material with gel-like physical consistency. Each capacitor configuration used a varying number and size of holes in the plastic sheet to create a variable "Percent Effective Area" (PEA) seen from the top electrode to the bottom. Experiments were designed to allow tests of capacitance, dielectric constant, energy density and power density for a variety of discharge times (frequencies of charge/discharge cycles). These four parameters were assessed for a frequency range across several different capacitor configurations using the constant current method as described. Additionally, a "Fast-Hold-Slow" (FHS) cycling method was used for select capacitors to further investigate the method itself as well as claimed performance benefits. Each configuration underwent numerous rounds of Normal Frequency and (some) FHS testing to aggregate and average data to ensure accurate and precise measurements.

B. CAPACITOR FABRICATION PROCEDURES

1. Thin PSDM Design and Test Matrix

The general concept for the thin PSDM form factor capacitors is to coat an electrode with a thin layer of the PSDM gel, and give the overall dielectric medium structure by inserting a non-conducting plastic membrane with holes interspersed. A schematic view of the overall design is seen in Figure 8.

The plastic was cut to a slightly larger size than the electrodes to help prevent edges of the electrodes from touching each other and shorting the circuit.

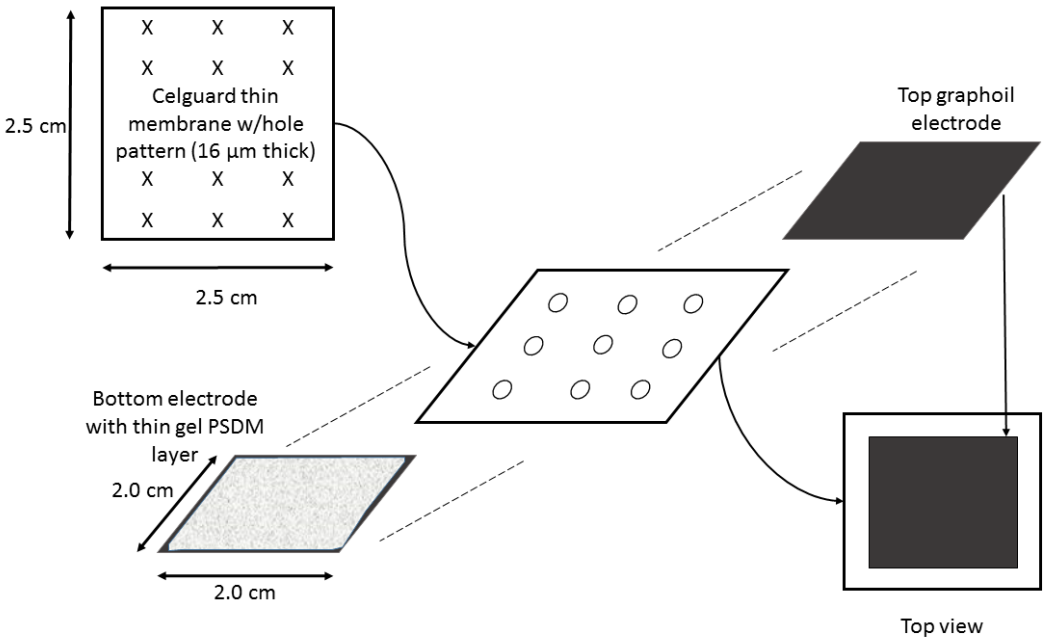

Figure 8. General PSDM Architecture

In total, there were a total of five hole-pattern configurations tested. Each hole pattern tested had a larger relative percentage of the total electrode surface area "exposed." That is, the holes in the membrane represent the effective surface area seen that can act as a capacitor. Because the electrodes for all cases were cut to 2.0 cm x 2.0 cm squares, the "Percent Effective Area" tabulated gives the proportion of open hole area to the effective 4.0 cm^2 total electrode area. Table 1 lists the different patterns used during experimentation:

Table 1. Thin Membrane Hole Configuration Test Matrix

Hole Diameter (mm)	Number of Holes	% Effective Area (PEA)
2.5	4	4.9
2.5	9	11.0
2.5	16	19.6
0.1	≈5900	46.5
2.5	≈FCC packing*	63.7

* Typical FCC packing densities for atoms are approximately 74%. However, due to the practical limitations of the laser cutter and general mechanical structure of the plastic insert, the highest measured PEA for this "FCC packing" design was ≈63.7%

The material used for this thin membrane is Celgard PP1615 Microporous Membrane. The technical data specifications are given in Table 2.

Table 2. Celgard® PP1615 Technical Data. Source: [27].

Basic Film Property	Unit of Measure	Typical PP1615 Value
Thickness	μm	16
Porosity	%	42
TD Tensile Strength	Kg/cm^2	150
MD Tensile Strength	Kg/cm^2	1560
Puncture Strength	Grams Force (gf)	280

2. Thin PSDM Fabrication Procedures

To build these five capacitors, the following procedures were used. In each step, careful attention was paid to measurements and recorded in log books. The following procedures were used in sequence. In most cases, multiple capacitors of the same hole design were made and tested, providing for more data to be analyzed and chosen as most representative of the general PSDM behavior in all tested cases.

a. STEP 1: Perform Necessary Cutting

A laser cutter was used to make precise cuts through the Celgard PP1615 Microporous Membrane in the hole arrangement and dimensions given in Table 1. Figure 9 shows the laser cutter while in operation cutting out a few inserts at once.

Additionally, 2.0 cm x 2.0 cm square electrodes were cut from grafoil, a commercially available paper-like material comprised primarily of graphite flakes.

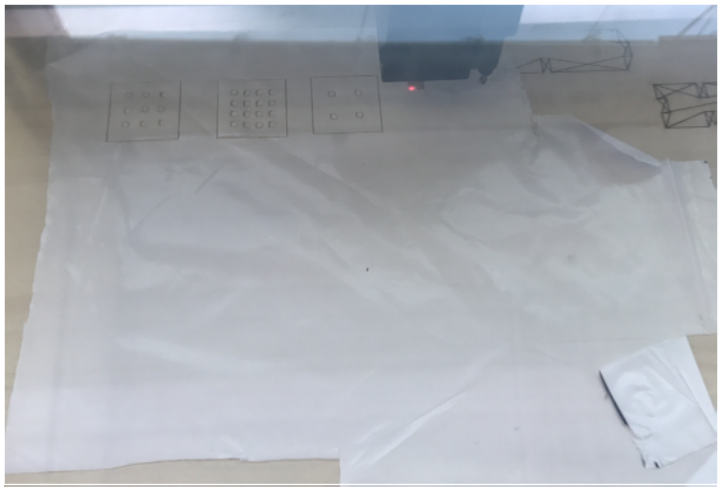

Figure 9. Laser Cutting Making Cuts through Membrane

b. STEP 2: Create PSDM Gel

In order to create the PSDM gel, the following were measured with a lab balance:

1. 1.38g of sodium chloride (Sigma Aldrich 10 mesh anhydrous beads, 99.999% NaCl, St. Louis, MO, USA)
2. 5.40 g DI H_2O
3. 0.61 g Fumed Silica (Sigma Aldrich, 0.007µm avg. particle size, St. Louis, MO, USA)

This ratio was chosen based on previous work wherein it was determined this ratio qualified the fumed silica, a very hygroscopic material, to have reached a point of "incipient wetness" [24].

Upon being thoroughly mixed, the following gel should appear as such depicted in Figure 10.

Figure 10. Fumed Silica PSDM Mixture after Mixing

c. STEP 3: Apply PSDM Gel and Assemble Capacitor

Next, a light coating of gel is applied to the bottom 2 cm x 2 cm grafoil electrode. Then, the appropriate Celgard membrane with holes cut is laid on top. Some examples are shown in Figure 11:

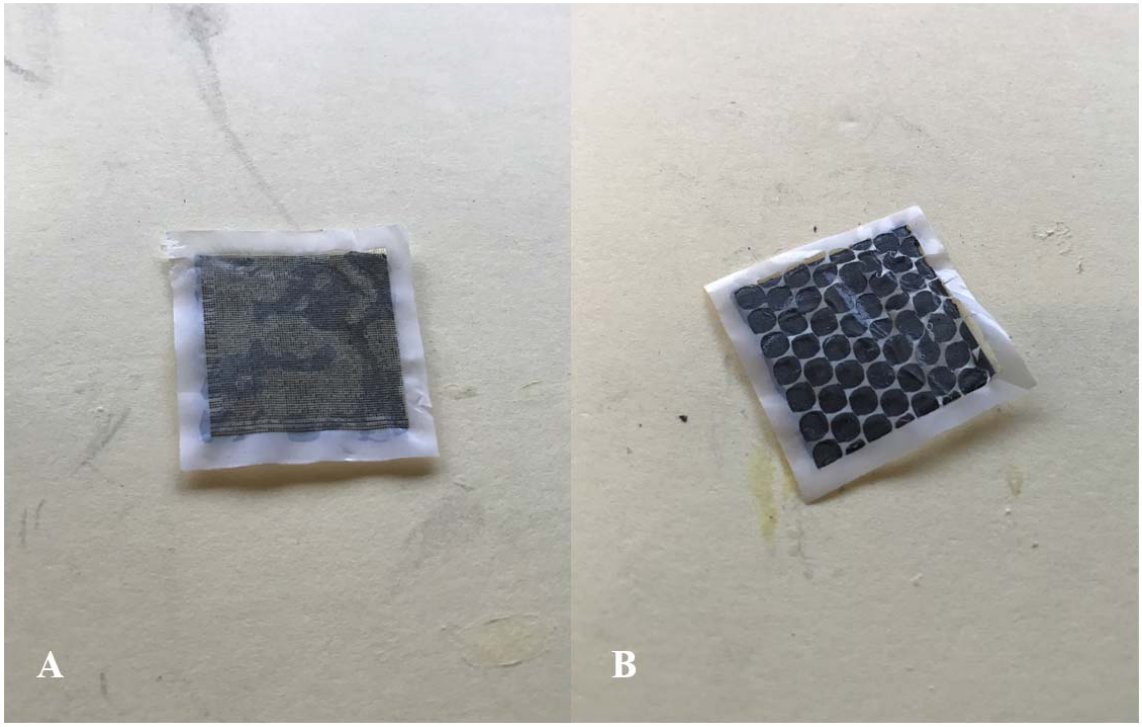

A: “Many” Hole design membrane over gel layer and bottom capacitor / B: FCC hole design in the same configuration

Figure 11. Examples of Capacitors before Top Electrode Is in Place

An assembled capacitor with the top electrode in place is shown in Figure 12. Once in place, a small 5.0 gram weight was gently placed across the top electrode to evenly squeeze and remove any gel from the capacitor to ensure a uniform thickness on the order of the thickness of the membrane (where the gel is occupying the space where the holes are cut).

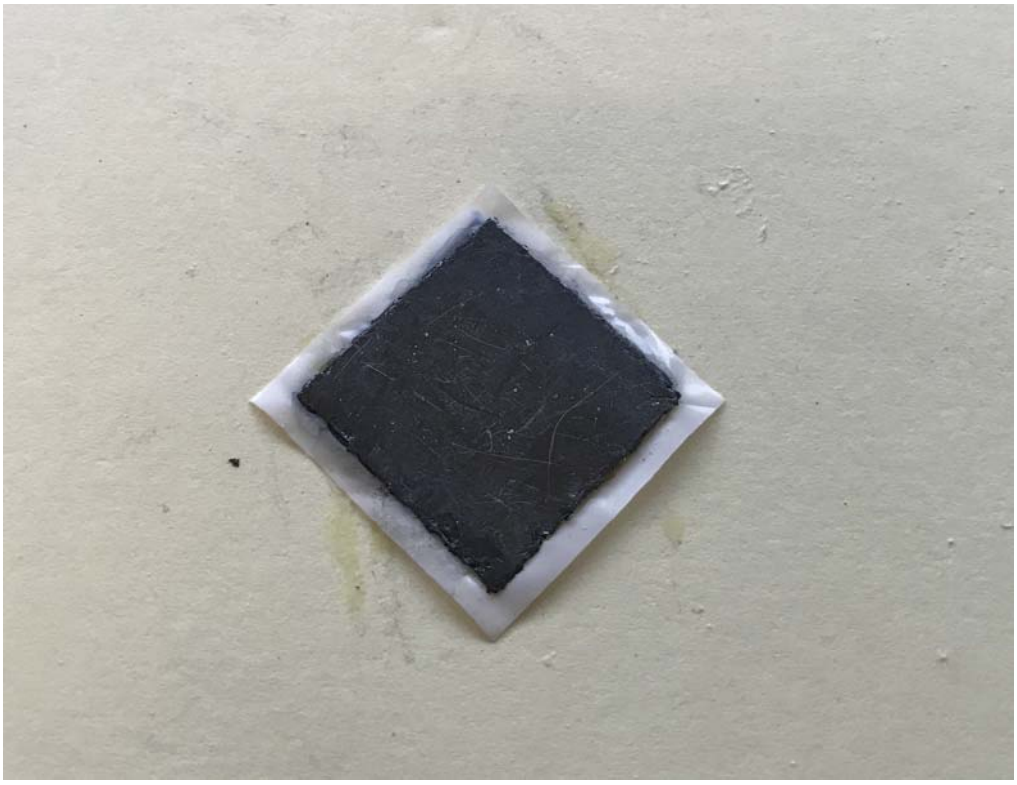

Figure 12. Fully Assembled Thin PSDM Capacitor (top view)

d. STEP 4: Assemble Capacitor Apparatus for Connection to VSP-300

Once the capacitor has been fully assembled, the grafoil leads were place on top and bottom before being sandwiched between two glass slides, held together by two small binder clips on either end. Tissue paper was wetted with DI water to help maintain relative humidity in the test chamber and to prevent too much deflection of the glass slides. This setup ensured good compression on the capacitor to ensure uniform thickness across the entire area. This is shown in Figure 13.

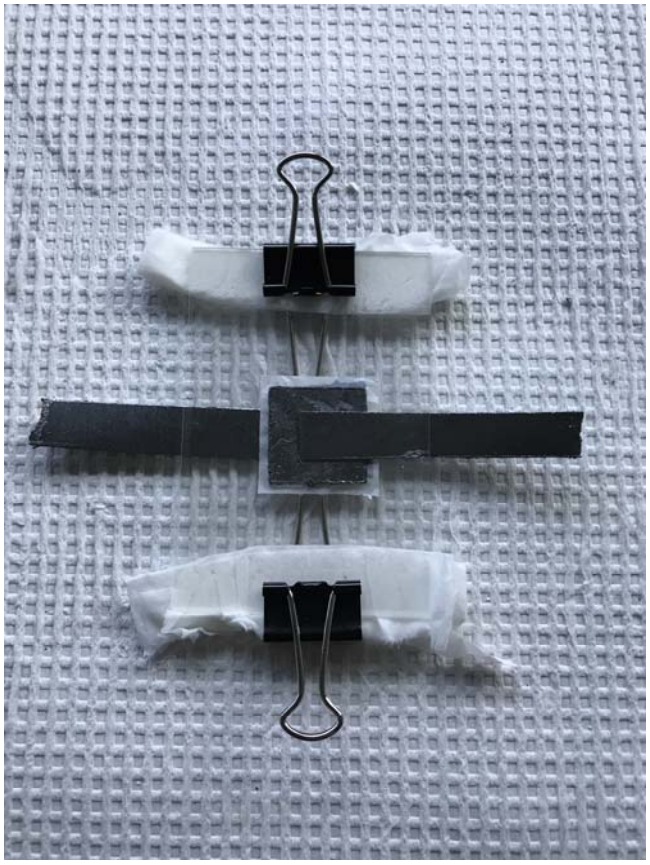

Figure 13. Capacitor Testing Apparatus with Grafoil Leads in Place

Lastly, the testing apparatus was connected to the Bio-Logic galvanostat via the grafoil leads for testing.

C. EXPERIMENTATION

1. Galvanostat Test Apparatus Setup

The Bio-Logic VSP 300 (Bio-Logic Science Instruments SAS, Claix, France) system was used in conjunction with the EC-Lab V11.02 software in order to conduct tests of the various thin PSDM capacitor designs. Figure 14 shows an up-close view of the capacitor setup connected back to the VSP 300 system, within the plastic environmental barrier.

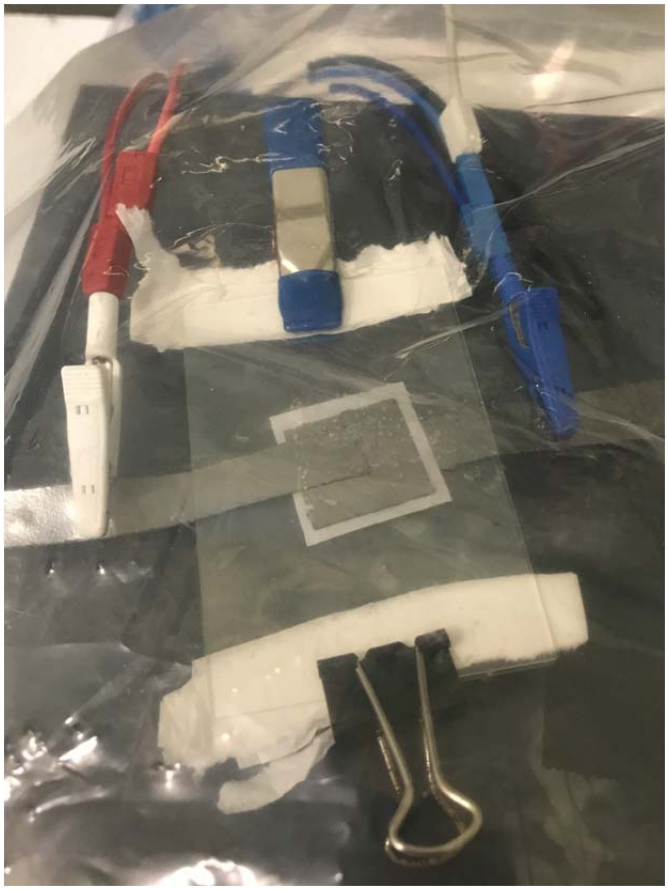

Figure 14. PSDM Capacitor Connected to the VSP 300 Leads Ready for Testing

2. EC Lab Software Setup

The EC Lab Software is used to set the parameters of each run of an experiment. A more detailed walkthrough of this step-by-step process is outlined by Lombardo [24], and exact file settings are found in the working group laboratory logbooks. In general, the technique settings follow the parameters listed in Table 3. Each capacitor was run according to these parameters. Note that all capacitors, in all cases, were charged to a maximum voltage of 2.3 V before being allowed to discharge. In the FHS trial sets, however, capacitors were set to charge to 2.3 V, kept that voltage for a period of time as described in Table 4, then allowed to discharge.

Table 3. Normal Frequency Charge and Discharge Schedule

Test Number	Charge Rate [mA]	Discharge Rate [mA]
1	2	2
2	3	3
3	5	5
4	10	10
5	15	15
6	25	25
7	40	40
8	60	60
9	75	75

Table 4. FHS Method Charge and Discharge Schedules

Test Number	Charge Rate [mA]	Hold Time [s]	Discharge Rate [mA]
	4 Hole Configuration		
1	5	300	0.5
2	5	600	0.5
3	5	900	0.5
	FCC Configuration		
1	7	300	4
	Many Hole Configuration		
1	15	300	3
2	15	600	3
3	15	900	3

3. Post-Test Analysis

Using a MATLAB script to pull data values out of the exported EC Lab .txt files, (as seen in Appendix A), the data for each Normal Frequency and FHS test was aggregated and analyzed. Results were plotted with MS Excel.

III. RESULTS

A. OVERVIEW

Overall, the results from each test Experiments conclusively demonstrated qualitative agreement with the central hypothesis of this thesis: the capacitance, dielectric constant, as well as energy and power densities increase as the PEA increases.

Note that the reported data points in fact represent an average across multiple trials of the same frequency, ensuring most accurate reporting of characteristic behaviors for these thin PSDM capacitors.

Additionally, it should be noted that for all data points collected with Average Discharge Times (ADT)s <0.001s, data was deemed "unreliable" given known measurement limitations of the VSP-300. While this machine is capable of sampling at extremely high rates and thus reports values on time scales well below 0.001s, parameters set for the trial runs in this research did not sample below that. This consideration is demarcated on the following graphs with a labeled line.

For dielectric constant, energy density, and power density calculations two results are reported. The first bases calculations off of the entire electrode area of the capacitor (4 cm^2 in all cases), as if the entire area were being used. These results, seen in Figures 15, 16, 18 and 20, are representative of how the entire capacitor performed. They are, however, conservative especially at the lowest PEA designs when much of that electrode area does not contribute to actual energy storage. The second set of results, seen in Figures 17, 19, 21 and 22, is based on only PEA which leads to conclusions centered on how the dielectric itself is actually operating. These results are less conservative, yet provide a more meaningful insight into the intrinsic PSDM characteristics over the set of tested cycling techniques (both normal frequencies and FHS in select cases).

B. NORMAL FREQUENCY PROTOCOL

In this section, the normal frequency results are presented and explained, for both total-area-based and PEA-based calculations.

1. Capacitance Results

Capacitance results were calculated based on the generally linear trend in discharge rates for capacitors below the 0.8 V threshold used in previous PSDM studies [24].

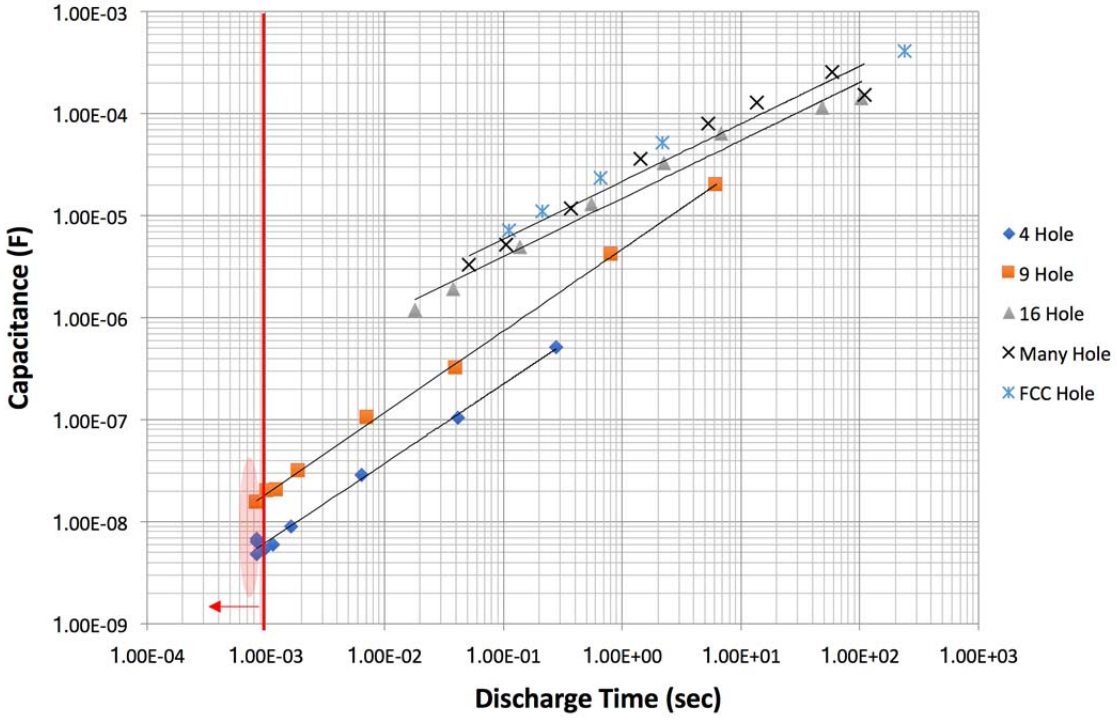

Figure 15. Normal Frequency Capacitance Results

As expected, a greater PEA leads to a higher capacitance at all discharge times. Also, as anticipated based on SDM theory and prior results longer discharge times also generally yield higher capacitance values in a given thin PSDM design. Finally note the "roll off" with decreasing discharge time curves are nearly parallel to the 4 and 6 hole cases but less sharp for the three capacitors with higher PEA values.

2. Dielectric Constant Results

Presented next are the dielectric constant results for both the total area and PEA-based calculations.

a. Total Capacitor Area-Based Calculations:

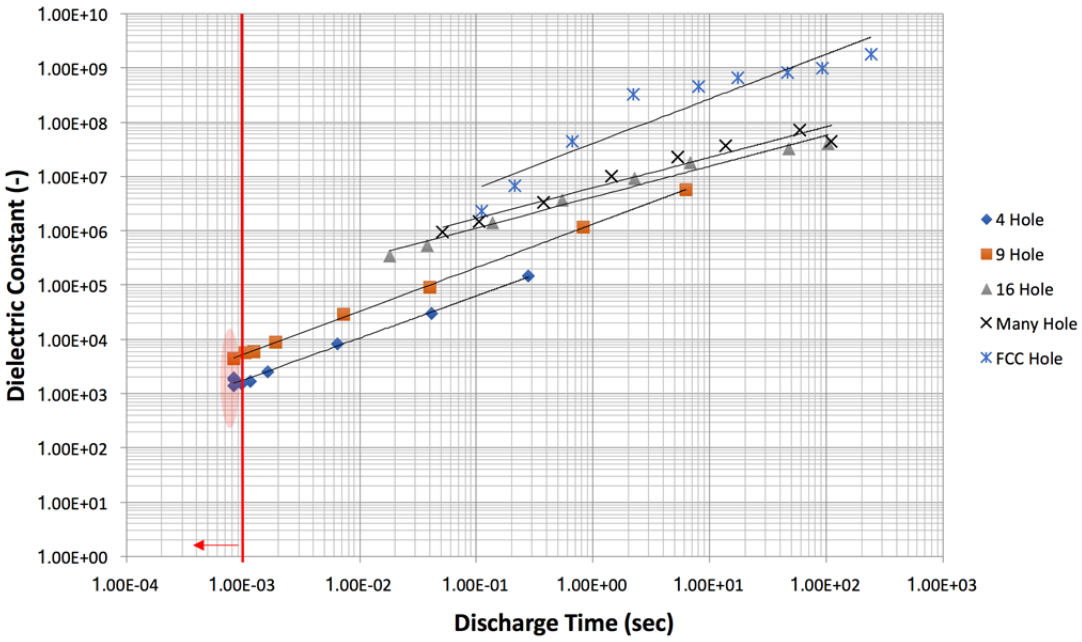

Figure 16. Normal Frequency Dielectric Constant Results (total area-based)

As expected, a greater PEA demonstrates dielectric values across discharge times, while longer discharge times also generally yield higher dielectric values in a given thin PSDM design. The dielectric constants were only determined below 1 volt, reflecting the fact that capacitance and dielectric constant decrease with voltage above ~1 volt. Once again, the roll-off for each type of capacitor is very linear, providing evidence that the data is "intentionally consistent." One investigating note is that the highest PEA samples has a slightly different roll-off pattern.

b. Percent Effective Area-based results

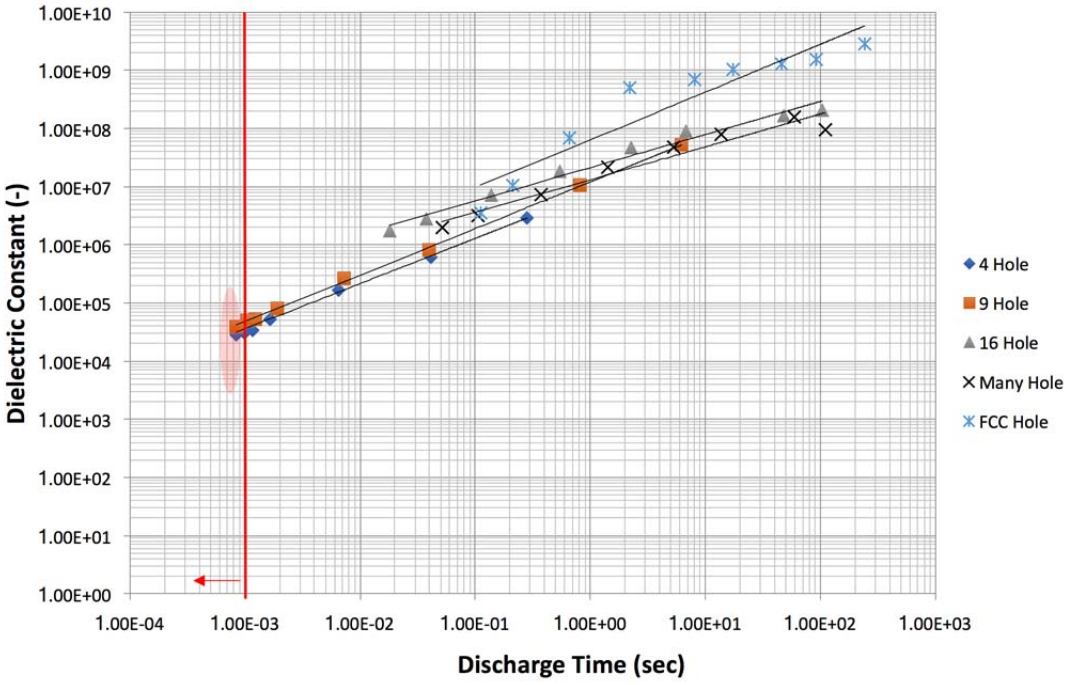

Figure 17. Normal Frequency Dielectric Constant Results (PEA-based)

The PEA-based calculations for dielectric constant show largely similar trends across designs and discharge times, albeit slightly higher values. If the dielectric constant, <1 volt, is only a function of PEA, all data could be plotted along a simple line. In fact, all data nearly does along a straight line with the exception of the capacitor with the highest PEA. In sum, the data suggests properties are characteristic of PEA only until a very high PEA is reached and do not depend on the number of holes cut in the polymer membrane. This concurs with the mathematical approach given that the PEA-based calculations consider only activated dielectric material contributing to the energy storage operation of the capacitor.

3. Energy Density Results

Energy density results were calculated based on the integrated area under the voltage vs. time discharge graph for each capacitor being cycled. The results are presented for both total capacitor area-based and PEA-based calculations.

a. Total Capacitor Area-Based Results

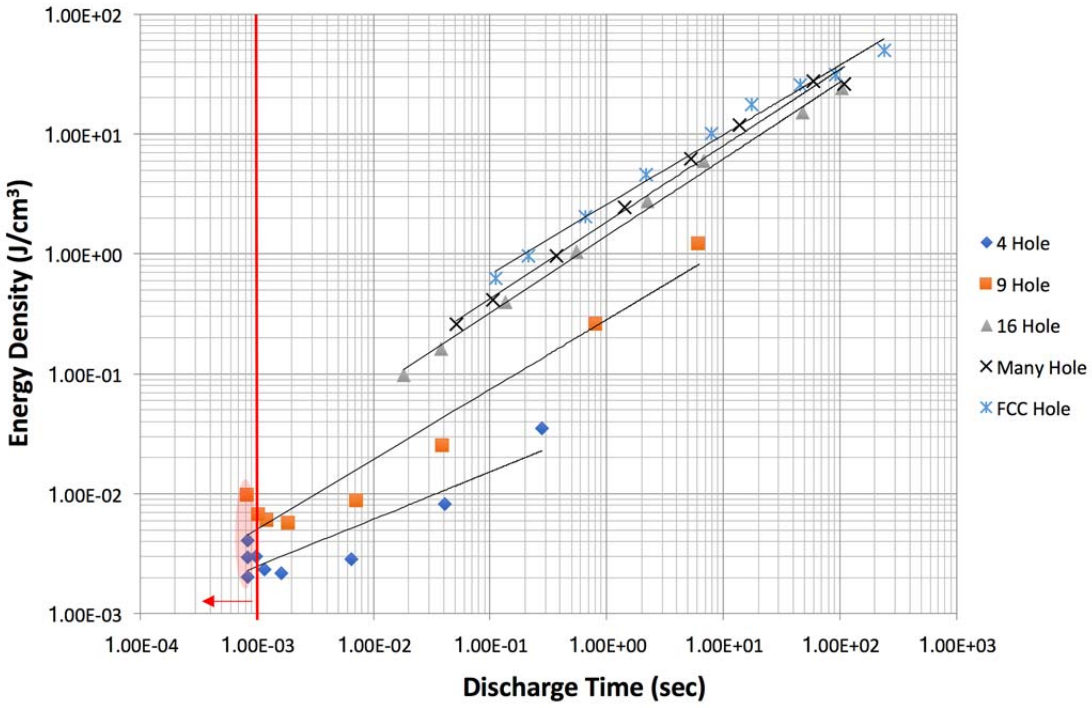

Figure 18. Normal Frequency Energy Density Results (total area-based)

Among each hole configuration, the frequency analysis clearly showed that higher energy densities are achieved at lower frequencies. This agrees with the previously studied SDM model, as longer discharge times more readily provide for the time-dependence SDM characteristics to be maximized where the dipole reorient.

Additionally, these results show that with an increasing PEA, absolute energy density also increases.

b. Percent Effective Area-Based Results

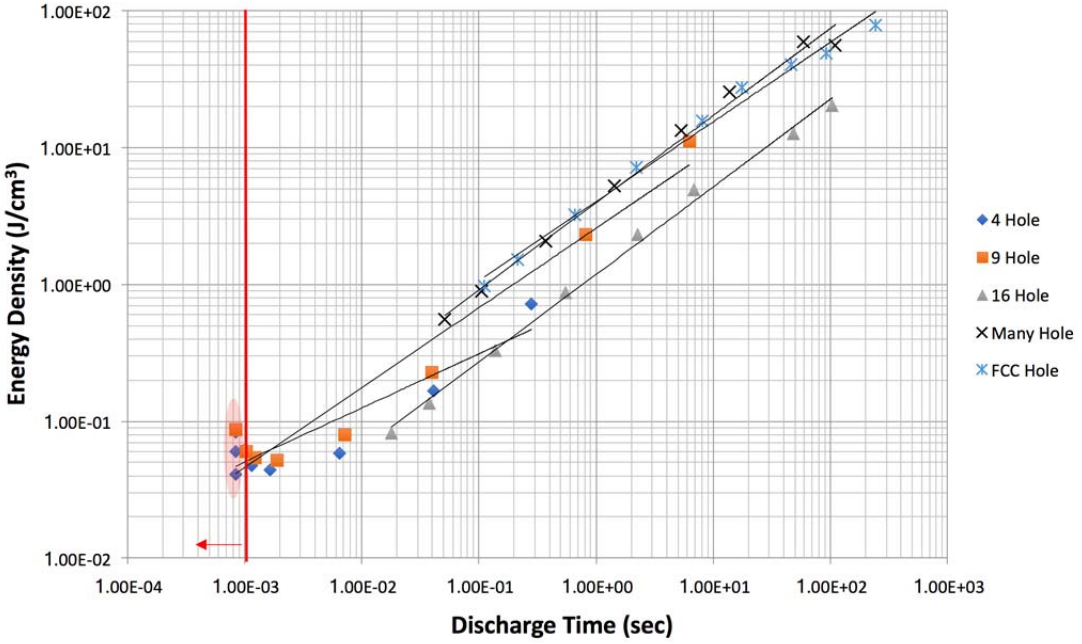

Figure 19. Normal Frequency Energy Density Results (PEA-based)

Among each hole configuration, the normal frequency analysis revealed that on a PEA-based energy density calculation, energy density similarly grows with longer discharge times. Key differences, however, demonstrate that this more material-specific calculation better highlights the potential of this material in thin form factors. At the longest discharge with the greatest PEA, these thin layer PSDM capacitors can reach energy densities up to 85 J/cm^3. This suggests that at these charging/discharging frequency rates, a capacitor built with a similarly thin layer of PSDM and potentially different hole geometries, energy densities up to this value or higher can be achieved across the entire capacitor volume. It is observed and noted that the 16 Hole data is uncharacteristically lower than the 4 or 9 Hole configurations for reasons unexplained by the simple SDM theory.

c. Energy Density Results Trends Versus PEA, on PEA-based Calculations

To better visualize how energy density varies with the various PEA's employed in this study, they are plotted against PEA for a given average discharge time (ADT), as seen in Figure 20:

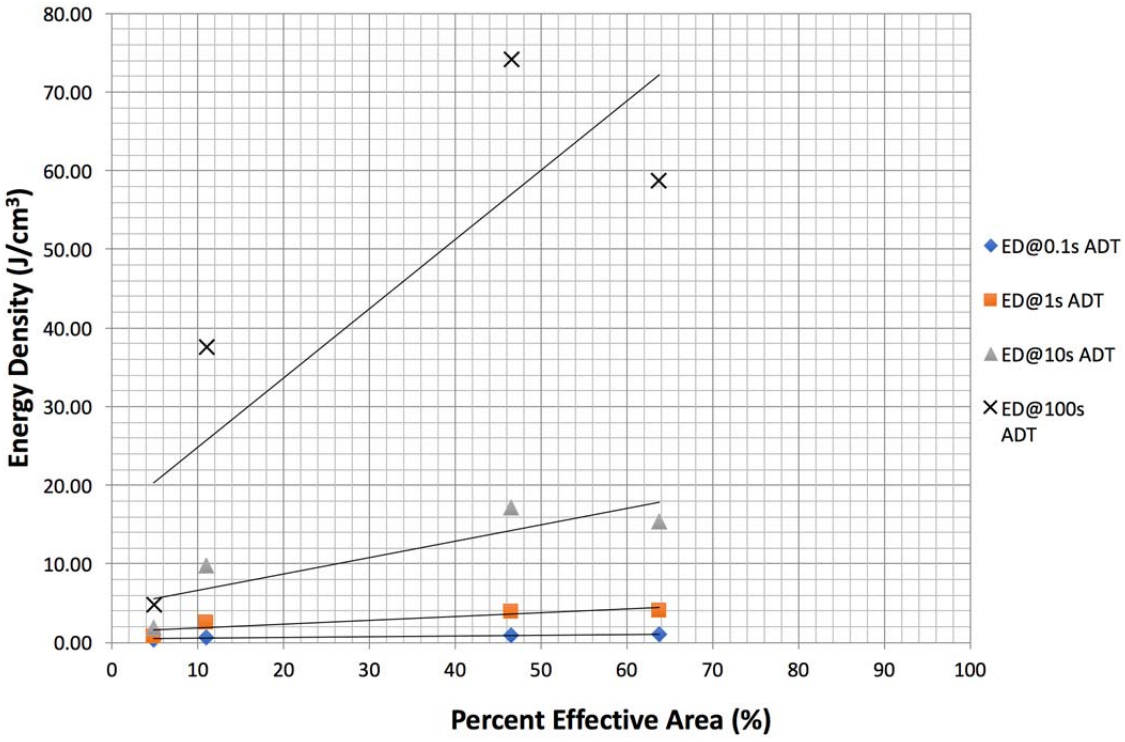

Figure 20. Energy Density vs. PEA for given ADTs

Here again, results are consistent with that of the other graphical representations. Greater energy densities are known to be seen with longer discharge times moving up the graph, and that upon removing the total area and basing energy density values solely on the activated PSDM contributing to energy storage, energy densities are largely linear across PEA designs actually used. The one deviation from this trend occurs at higher ADTs which—coupled with a higher energy density reported for the 46.5 PEA versus the 63.7 PEA at the same ADT—suggests a small geometric effect in hole density may exist.

4. Power Density Results

Power density results were calculated based diving the energy density values by the average discharge time, giving energy density per time (power). The results are presented for both total capacitor area-based and PEA-based calculations.

a. Total Capacitor Area-Based Results

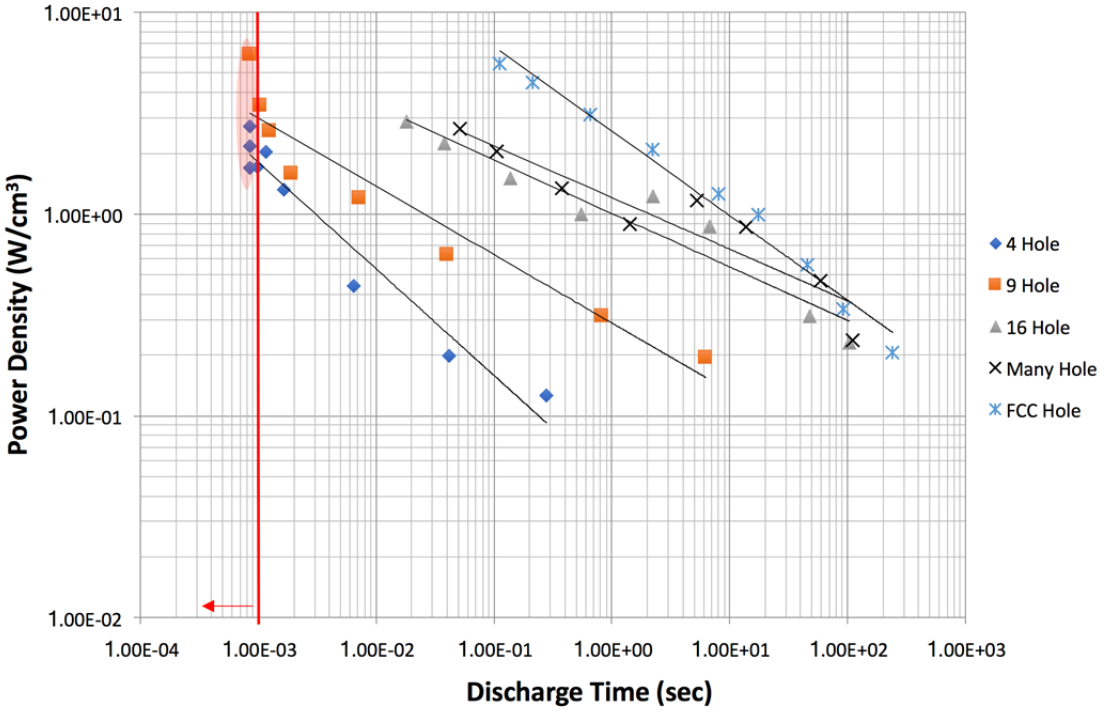

Figure 21. Normal Frequency Power Density Results (total area-based)

Conversely, longer discharge times inhibit power density performance among capacitors of the same design. Shorter discharge times (i.e., higher frequencies) reveal better power densities across all hole configurations.

Additionally, it should be noted that as PEA increases, very short discharge times could not be achieved for the same high discharge current (e.g., 75 mA) at which the other capacitors were tested. However, trends shown above extrapolated to very short discharge times reveal potentially astonishing power density values (i.e., >100 W/cm^3).

Tests at higher discharge currents for high PEA capacitors should be performed to validate this empirically.

b. Percent Effective Area-Based Results

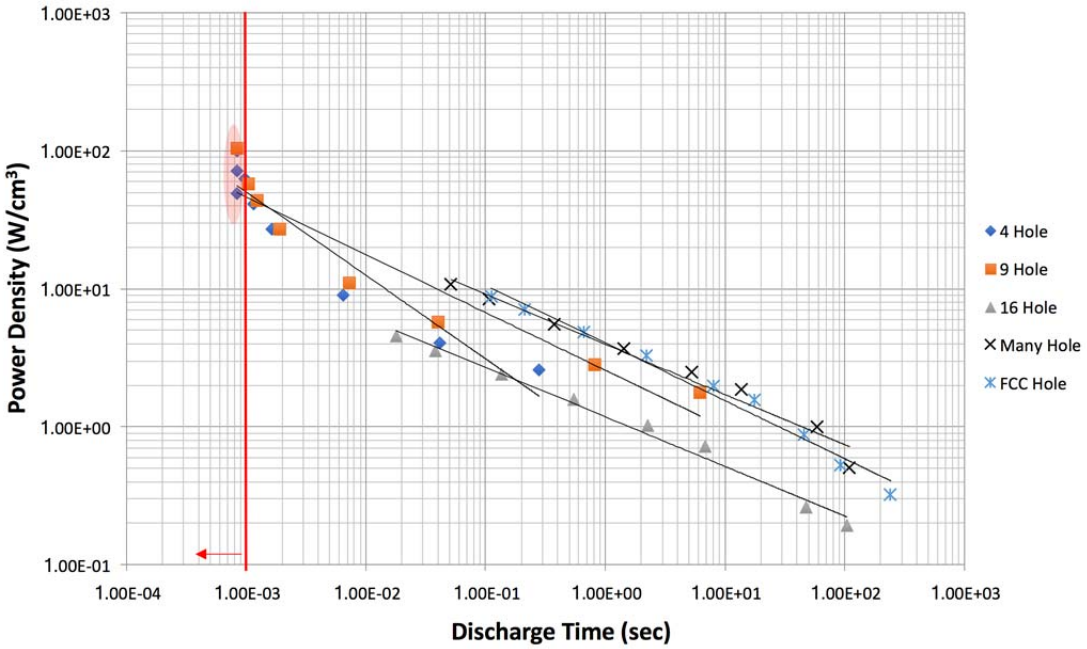

Figure 22. Normal Frequency Power Density Results (PEA-based)

A relatively close grouping of power density values all on similar trend lines give further credence to the characteristic power density behavior of these thin PSDM capacitors at different frequencies. Similar to the PEA-based energy density numbers, it is observed and noted that the 16 Hole data is uncharacteristically lower than the 4 or 9 Hole configurations for reasons unexplained by the simple SDM theory.

C. FHS PROTOCOL RESULTS

Only incomplete comparisons can be made among the capacitor designs for the FHS results, as charge and discharge parameters could not remain constant to yield improved results over normal frequency testing, and in some cases, did not yield improved results similar in trend to the normal frequency results (Table 5). For instance,

the Many hole design's FHS results greatly surpassed that of the FCC FHS results. Moreover, as mentioned, this is not a truly complete comparison as frequency parameters such as discharge current were nonstandard across FHS testing due to capacitor limitations (some could not continue to cycle after extremely long (>300 sec) discharge times).

Table 5. FHS Results Summary for Two Thin PSDM Capacitors at Recorded Discharge Times

	PEA (%) / ADT (s)	4.9% / 97.8 s	46.5% / 343s
PEA-based Results	Capacitance (F)	8.85E-02	1.05
	ε	8.17E+09	1.02E+10
	Energy Density (J/cm^3)	44.7	195
	Power Density (W/cm^3)	0.456	0.567

However, in the context of a single capacitor design the FHS method produced the best results. More specifically, they typically produce values that can be as little as 30% better in the Many Hole case, and as much as 800% better in the 4 Hole case under (low) frequency response testing. Clearly then, eventual fielded use of these types of capacitors should, where possible, attempt to use this charging and discharging method. This is not unrealistic in most typical circumstances where weapons are intended to engage one or two targets per engagement. Should the need for more rapid discharge cycling arise, optimal performance will suffer but functionality will not be lost altogether. Furthermore, depending on the weapon specifics, it may be possible to fire many "shots" per given charge.

IV. DISCUSSION

A. EMPIRICAL FINDINGS

Empirical findings for capacitors support the existing PSDM, and can now help assert that the model applies to PSDMs applied at thinner layers, and operated over a range of charging/discharging frequencies.

B. THIN PSDM OUTCOMES

There are five important empirical outcomes, all consistent with the Hypothesis and the expected behavior based on SDM theory and earlier results on other types of SDM form factors.

1. Thin Form Factors Work

As suggested by previous results from work with PSDM at thicknesses >300 μm by Jenkins, Petty, and Phillips, decreasing dielectric thickness may result in superior capacitance, dielectric constant, energy density and power density values [24]. The results of this research empirically prove that previous PSDM models not only work with thin form factors, but also indicate the dielectric values do retain the same characteristics reported in earlier studies (e.g., 10^9 at a 10 second discharge time) based on thick layers of fumed silica saturated by NaCl solutions. Thus the "dielectric values" can be used to predict energy densities to thicknesses of 16 μm, and perhaps the model can extend to even thinner layers of PSDM as well. This also leads to questions about whether the model holds at sub-micron thickness, and if so, what manufacturing methods might apply while maintaining the cheap material and inexpensive fabrication method priorities.

2. PEA Trends

The primary parameters used to measure the overall performance in this thesis all show logical, linear trends with respect to increasing PEA. Measured energy density, power density, capacitance <1 volt, and dielectric constants all increased as open area increased. The degree to which these metrics increased was also generally linear,

however, practically achieving hole geometries for PEA's >65% will be challenging using methods presented in this research. In several cases, the "Many" hole design actually performed slightly better than the "FCC" design, suggesting that more, smaller holes may in fact perform better than a larger, less structured film matrix with a higher PEA.

All findings also supported the intrinsic nature of the PSDM characteristics, thereby extending previously developed models to newly attained sub-20 micron thicknesses.

3. Consistent Discharge and Frequency Behavior

It should be noted that the consistency in both discharge behavior and frequency response is increasingly important to the overall SDM model development which is a laborious, ongoing process. Both behaviors provide for log-log plots of pertinent data with which trends in previous studies can be directly compared. These trends are helpful not only in each specific case, but also in prediction of unstudied behaviors to test model consistency. These in turn contribute to our greater understanding of SDMs and how they might eventually prove to be part of the solution to the Navy's energy density storage problem.

In the case of thin PSDM capacitors, the slope of the discharge curves across the entire voltage range (0-2.3 V) is consistent with that of previous PSDM studies [13]. Furthermore, the frequency roll-off of capacitor performance values at high frequencies is also consistent with that of previous studies.

Taken together, consistency in discharge and frequency behaviors at thin layers of PSDM suggest that it may be fruitful to explore even thinner layers of PSDM.

4. Commercial Supercapacitor Comparison

Of note, these thin PSDM capacitors compare quite favorably with today's commercially available supercapacitors. The energy density of the PSDM with the ~64% open area (90 J/cm^3) was ~3x better than the best commercial supercapacitor for long discharge times [22]. What is more, the full data set results for energy density over a

variety of frequencies is available, providing far more insight than simply quoting a capacitance rating without specifying the methods used to measure that value or the frequency response that capacitor might exhibit.

5. Geometric Effects

There are a few minor deviations to the trends in the data presented in this research. In each instance, the least convoluted explanation can be reasonably explained as possible geometry effects. While these trend deviations are never more than 10-15% of the expected value across all four key performance indicators, they are still noticeable to a degree. For example, upon closer inspection of Figure 20 it appears as if benefits for energy density of increasing PEA past 50% diminish slightly.

Some specific physics phenomena which fall under the general category of geometric effects and pertain specifically to the SDM model include edge effects and dipole proximity, each of which generally state that on dielectric layers of this scale, relative position of "holes" cut in the polymer film may affect the observed performance. The simple SDM dielectric theory does not fully account for these minor fluctuations as they have just been discovered and yet to be fully explored.

THIS PAGE INTENTIONALLY LEFT BLANK

V. CONCLUSIONS AND FUTURE WORK

A. CONCLUSIONS

Generally, thin Powder-based Superdielectric Material capacitors demonstrate that they are in fact feasible capacitor configurations for high energy density storage. Specifically, results were shown to successfully fabricate a variety of thin PSDM capacitors with very thin films of aqueous NaCl solution saturated silica gel films spread within holes of a very thin (16 μm) polymer sheet. By varying the given "effective area" used per capacitor configuration, this study showed that better the overall performance is achievable in all four primary capacitor metrics: capacitance, dielectric constant, energy density and power density.

When the four primary metrics were assessed on a total capacitor area- and percent effective area-basis, additional insight was provided for how these novel capacitor form factors work in an engineering sense, as well as intrinsically on a material basis alone. Both sets of results contribute to our level of understanding for what PSDM capacitors are capable of presently, as well as provide clues as to what avenues of future research should be explored to further expand the SDM model in as many dimensions as possible.

Additionally, the incorporation of the FHS technique into this research was particularly enlightening in two key ways. First, it is clear FHS cycling do provide insight into a specific capacitor's theoretical maximum performance. The second learning, however, prompts caution when attempting to draw conclusions about trends in FHS results across different capacitors. That is, different capacitor designs required slightly different implementations of the FHS method and thus cannot be as easily compared as it might appear. Furthermore, requiring FHS cycling to attain optimal performance may be unnecessarily prescriptive in the Navy's context and thus may not be truly representative of the capacitor operation in everyday use.

In summary, this research endeavor successfully pushed the bounds of superdielectric materials, and will provide the basis for much promising PSDM work to follow.

B. FUTURE WORK

More work can be done to further the already promising results demonstrated in this thesis. Future endeavors in this research should seek to answer the following questions:

1. Can this thin PSDM form factor be scaled to even thinner dielectric constant layers? If so, are there frequency impacts? Performance impacts?

This may be one of the main advantages of using fumed silica versus other nonconducting porous media used in earlier studies because, as stated in the procedures, the fumed silica particles are measured to be on the order of nanometers in diameter. Consequently, thin layer on the orders of hundreds of nanometers are, in fact, feasible than if particles that already had diameters on the micron scale.

2. In reference to the geometry effects, can different permutations and combinations of large and small holes be optimized?

Perhaps holes of various sizes can be used to make more efficient use of unused space on the membrane, further increasing PEA. Caution must be taken to ensure structural integrity of the membrane post-cutting and may meet limitations due to laser cutter tolerances.

3. Are there other methods to improve the max charge voltage? Would a different electrolyte that is not water-based (aqueous) surpass the breakdown voltage of water and allow for a max charge voltage higher than 2.3 volts?

Presently, there was some limited success demonstrated in concurrent TSDM research with different organic electrolytes which may prove fruitful should high enough concentrations of salt be dissolved in said solutions. Principally, whatever means exist to increase the concentration of dipoles to the maximum extent possible while avoiding the use of water as the solvent of ionic compounds will succeed at this task, and presumably could be implemented in the powder SDM work.

APPENDIX A. MATLAB SCRIPT FOR DATA ANALYSIS

```
%=========================================================================
% Script name:      Voltage Data Analysis
% Written by:       ENS Mitchell T. Heaton + LTJG Clayton W. Petty
% Last modified:    16 MAY 2017
% Disclaimer:       MODIFY AT YOUR OWN RISK!!!
%=========================================================================
% Reads in a series of text files to observe voltage cycling with
respect
% to time. Separates the data into distinguishable series with start at
% peak voltage and end at minimum voltage before the charging process
% reinitiates.

% INPUT ARRAYS:
%   *.txt file
%
% OUTPUT ARRAYS:
%   fileMetrics[File #, C, Epsilon, ED, PD, ADT]
%
%=========================================================================
%=========================================================================
%% Workspace Cleanup

clc
clear
close all
format compact

%=========================================================================
%% Multi-file Read In

% Specify the folder where the files live
%Must be adjusted every time run!
myFolder = 'thesis_data/XXXX'; % ex. 'folder/subfolder/NormFreq1'
% Check to make sure that folder actually exists.  Warn user if it
doesn't.
if ~isdir(myFolder)
  errorMessage = sprintf('Error: The following folder does not
exist:\n%s', myFolder);
  uiwait(warndlg(errorMessage));
  return;
end
% Get a list of all files in the folder with the desired file name
pattern.
filePattern = fullfile(myFolder, '*.txt');
theFiles = dir(filePattern);
for k = 1 : length(theFiles)
  baseFileName = theFiles(k).name;
  fullFileName = fullfile(myFolder, baseFileName);
  %fprintf(1, 'Now reading %s\n', fullFileName);
end


%=========================================================================
%% General Information

% Givens variable establishment
```

```
k = 9; % NormFreq=9 / FHS=3 %OR PROMPT by: input('How many files are in
this folder?');
prompt = {'Enter measured capacitor area (cm^2):','Enter measured
capacitor thickness (cm):'};
dlg_title = 'Input';
num_lines = 1;
defaultans = {'4','0.0016'};
answer = inputdlg(prompt,dlg_title,num_lines,defaultans);
capArea = str2double(cell2mat(answer(1,1)));
capThickness = str2double(cell2mat(answer(2,1)));
epsilon0 = 8.85e-12; % Permissivity of free space (F/m)

% Vector initialization with respect to maximum bounds on cycles and
% numFiles

    maxCycles = 50; %max number of cycles in a given folder
    energyDensity = nan(k,maxCycles);
    capacitance = nan(k,maxCycles);
    epsilon = nan(k,maxCycles);
    intArea = nan(k,maxCycles);
    dischargeTimeVec = nan(k,maxCycles);

    fileMetrics = nan(k,6);

% Loop through all files in folder
for k = 1 : length(theFiles)
  baseFileName = theFiles(k).name;
  filename = fullfile(myFolder, baseFileName);
  fprintf(1, 'Now reading %s\n', filename);

    %filename = uigetfile('.txt','Select the file you would like to
import and analyze');

    disp('Importing text file of voltage data.')
    DataSet = readtable(filename);
    disp('Data import complete')

    voltageVec = table2array(DataSet(:,11))';
    timeVec = table2array(DataSet(:,9))';
    fid = fopen(filename);
    C = textscan(fid,'%s');
   A = C{1,1};
    index1 = find(ismember(A,'ctrl1_val'));
    chargeCurrent = str2num(cell2mat(A(index1+1)));
    dischargeCurrent = str2num(cell2mat(A(index1+2)))*(.001); %now in
[=] Amps

    %Max and min function recreated for .txt data
    maxPoints = [];
    minPoints = [];
    lastMin = 0;
    lastMax = 1;
    minInd = [];
    maxInd = [];

    for i = 2:length(voltageVec)
        prev = voltageVec(i-1);
        now = voltageVec(i);

        if i==2 % Initilization loop to establish if first point is
going to be considered a min or a max
            if prev < now
```

```
                minPoints = prev;
                minInd = i;
                lastExtrema = 'min';
            elseif prev > now
                maxPoints = prev;
                maxInd = i;
                lastExtrema = 'max';
            else
                disp('Beginning Point min or max undetermined in one
time step')
            end
        end

        if 1 == strcmp(lastExtrema,'min') && now > prev && now >
1.2*lastMin % Case 1: Coming from local minimum, new local maximum at
least 1.2 times greater than last local minimum
            newExtrema = now;
            maxPoints = [maxPoints,newExtrema];
            maxInd = [maxInd,i];
            lastExtrema = 'max';
            lastMax = now;
        elseif 1 == strcmp(lastExtrema,'min') && now < lastMin && now <
0.8*lastMax % Case 2: Coming from local minimum and looking for local
max...find a value lower than previous local minimum
            replaceExtrema = now;
            minPoints = [minPoints(:,1:(end-1)),replaceExtrema];
            minInd = [minInd(:,1:(end-1)),i];
            lastExtrema = 'min';
            lastMin = now;
        elseif 1 == strcmp(lastExtrema,'max') && now < prev && now <
0.8*lastMax % Case 3: Coming from local maximum, new local minimum at
least 0.8 times less than last local maximum
            newExtrema = now;
            minPoints = [minPoints,newExtrema];
            minInd = [minInd,i];
            lastExtrema = 'min';
            lastMin = now;
        elseif 1 == strcmp(lastExtrema,'max') && now > prev && now >
1.2*lastMin % Case 4: Coming from local maximum and looking for local
minimum...find a value greater thatn last previous local maximum
            replaceExtrema = now;
            maxPoints = [maxPoints(:,1:(end-1)),replaceExtrema];
            maxInd = [maxInd(:,1:(end-1)),i];
            lastExtrema = 'max';
            lastMax = now;
        end
    end

    minTimeVal = timeVec(minInd);
    maxTimeVal = timeVec(maxInd);
    figure()
    hold on
    xlim([minTimeVal(1,1)-
0.01*minTimeVal(1,1),minTimeVal(1,end)+0.01*minTimeVal(1,end)])
    ylim([minPoints(1,1)-
0.1*maxPoints(1,1),maxPoints(1,1)+0.1*maxPoints(1,1)])
    xlabel('Time (sec)')
    ylabel('Voltage (Volts)')
    plot(timeVec,voltageVec,'-k')
    plot(maxTimeVal,maxPoints,'*r')
    plot(minTimeVal,minPoints,'*g')
```

```
    %Data Analysis Portion
    %Set number of iterations in loop to number of discharges in given
file
    analysisPeaks = [maxPoints(1,2:end);minPoints(1,3:end)]; % Removes
the first charge and discharge from the area to be analyzed (makes
assumption that the capacitor starts uncharged (in removing first two
samplings on the minimum side, one on the maximum side)
    analysisInd = [maxInd(1,2:end);minInd(1,3:end)];
    numCycles = length(analysisPeaks);

    if numCycles == 0
        i=1;
        startVal = analysisPeaks(1,i);
        endVal = analysisPeaks(2,i);
        startInd = analysisInd(1,i);
        endInd = analysisInd(2,i);
        voltVecNow = voltageVec(:,startInd:endInd);
        timeVecNow = timeVec(:,startInd:endInd);
        dischargeTime = timeVecNow(1,end)-timeVecNow(1,1);
        intArea(k,i) = trapz(timeVecNow,voltVecNow);
        [garbage,regStart] = find(voltVecNow<0.8);
        regVoltVec = voltVecNow(1,regStart:end);
        regTimeVec = timeVecNow(1,regStart:end);
        guessdVdt = mean(diff(regVoltVec)./diff(regTimeVec)); %best way
to calc dVdt given type of data
%           %[p,s] = polyfit(regTimeVec,regVoltVec,1);
            %dVdt = p(1,1);
        capacitance(k,i) = (.001)*dischargeCurrent./abs(guessdVdt);
%puts C in Coloumbs
        epsilon(k,i) =
capacitance(k,i)./((epsilon0.*capArea*.0001)./dischargeTime);
        energyDensity(k,i) =
intArea(k,i).*dischargeCurrent./(capArea.*capThickness); %J/cm3
        powerDensity(k,i) = energyDensity(k,i)./dischargeTime; %energy
delivered per cycle [=] J/s/cm3
        dischargeTimeVec(k,i)= dischargeTime;

    elseif numCycles > 0
        for i=1:numCycles
            startVal = analysisPeaks(1,i);
            endVal = analysisPeaks(2,i);
            startInd = analysisInd(1,i);
            endInd = analysisInd(2,i);
            voltVecNow = voltageVec(:,startInd:endInd);
            timeVecNow = timeVec(:,startInd:endInd);
            dischargeTime = timeVecNow(1,end)-timeVecNow(1,1);
            intArea(k,i) = trapz(timeVecNow,voltVecNow);
            [garbage,regStart] = find(voltVecNow<0.8);
            regVoltVec = voltVecNow(1,regStart:end);
            regTimeVec = timeVecNow(1,regStart:end);
            guessdVdt = mean(diff(regVoltVec)./diff(regTimeVec)); %best
way to calc dVdt given type of data
    %           %[p,s] = polyfit(regTimeVec,regVoltVec,1);
                %dVdt = p(1,1);
            capacitance(k,i) = (.001)*dischargeCurrent./abs(guessdVdt);
%puts C in Coloumbs
            epsilon(k,i) =
(capacitance(k,i)./((epsilon0.*capArea*.0001)))/1000;
            energyDensity(k,i) =
intArea(k,i).*dischargeCurrent./(capArea.*capThickness); %J/cm3
            powerDensity(k,i) = energyDensity(k,i)./dischargeTime;
%energy delivered per cycle [=] J/s/cm3
```

```
            dischargeTimeVec(k,i)= dischargeTime;
    %         figure()
    %         plot(timeVecNow,voltVecNow,'-k')
    %         xlabel('Time (s)')
    %         ylabel('Voltage (V)')
    %         title(['Discharge curve for cycle ',num2str(i),' of the
given file'])
        end
    end

    %input file avg's in FILE_METRICS array
    % FILE_METRICS = [cap_avg, epsilon_avg, energyDensity_avg,
    % powerDensity_avg]
    fileMetrics(k,1) = k; %filenumber
    fileMetrics(k,2) = nanmean(capacitance(k,:)); %avg capacitance in
file
    fileMetrics(k,3) = nanmean(epsilon(k,:)); %avg epsilon in file
    fileMetrics(k,4) = nanmean(energyDensity(k,:)); %avg ED in file
    fileMetrics(k,5) = nanmean(powerDensity(k,:)); %avg PD in file
    fileMetrics(k,6) = nanmean(dischargeTimeVec(k,:)); %avg Discharge
Time in file

end

%% Hole Configuration Plots

%ED and PD vs. Avg Discharge Time
subplot(1,2,1);
    x = fileMetrics(:,6);
    y1 = fileMetrics(:,4);
    scatter(x,y1)
    title('Energy Density vs. Discharge Time');
    ylabel('Energy Density (J/cm^3)');
    xlabel('Average Discharge Time (s)');

subplot(1,2,2);
    x = fileMetrics(:,6);
    y2 = fileMetrics(:,5);
    scatter(x,y2)
    title('Power Density vs. Discharge Time');
    xlabel('Average Discharge Time (s)');
    ylabel('Power Density (W/cm^3)');
```

THIS PAGE INTENTIONALLY LEFT BLANK

APPENDIX B. SELECT HOLE PATTERN MICROGRAPHS

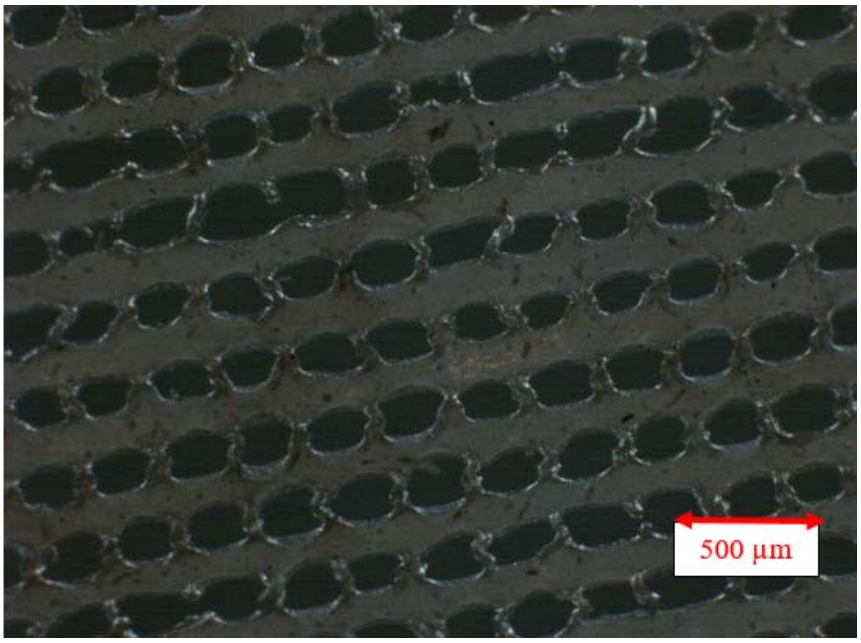

Figure 23. Lower Magnification View (5x) of the "Many" Hole Design

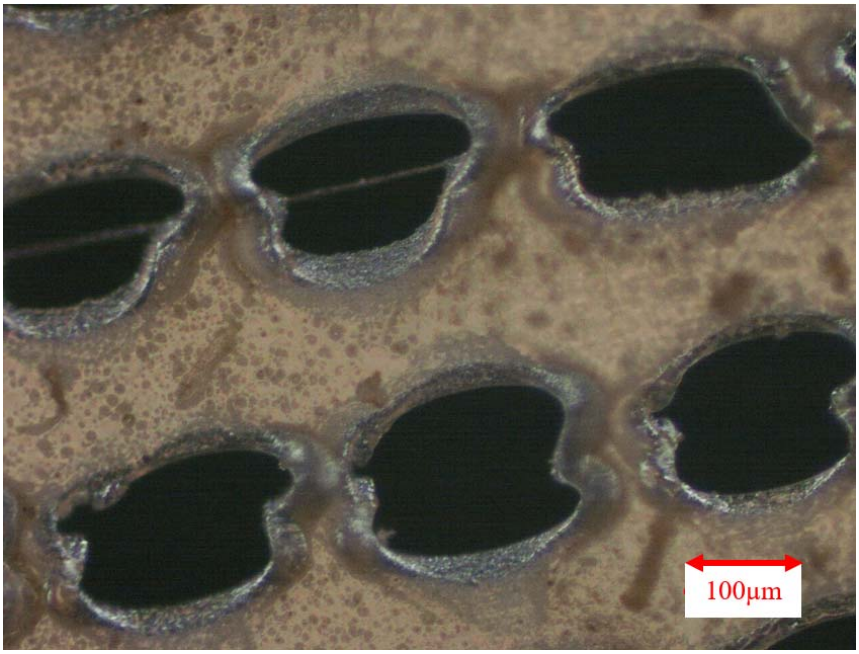

Figure 24. Lower Magnification View (10x) of the "Many" Hole Design

THIS PAGE INTENTIONALLY LEFT BLANK

LIST OF REFERENCES

[1] Maxwell Technologies, Inc. (2015). Maxwell Technologies ultracapacitors product comparison matrix. San Diego, CA. [Online]. Available: http://www.maxwell.com/images/documents/Product_Comparison_Matrix_3000489_2.pdf.

[2] V. R. Basam and A. Das, "All electric ship-the super platform for tomorrow's naval warfare," presented at the *Second International Seminar and Exhibition on Naval Armaments (NAVARMS),* January, 2010.

[3] T. Atwater, P. Cygan and F. Leung, "Man portable power needs of the 21st century - I. Applications for the dismounted soldier. II. Enhanced capabilities through the use of hybrid power sources," *J. Power Sources,* vol. 91, pp. 27–36, Nov 2000.

[4] J. Bennett. (2016, Jun. 6). The future of the Navy's electromagnetic railgun could be a big step backwards. [Online]. Available: http://www.popularmechanics.com/military/weapons/a21174/navy-electromagnetic-railgun/

[5] L. Lu, X. Han, J. Li, J. Hua, and M. Ouyang, "A review on the key issues for lithium-ion battery management in electric vehicles," *J. Power Sources,* vol. 226, pp. 272–288, Mar. 2013.

[6] A. J. Bard and L. R. Faulkner, *Electrochemical Methods and Applications.* Hoboken, NJ: John Wiley & Sons, 2001.

[7] J. R. Miller and A. F. Burke, "Electrochemical capacitors: challenges and opportunities for real-world applications." *The Electrochemical Society Interface,* vol. 17 (1), pp. 53-57, Spring, 2008.

[8] P. Simon and Y. Gogotsi, "Materials for electrochemical capacitors," *Nature Materials,* vol. 7, pp. 845-54, Nov 2008, 2008.

[9] M. C. Stewart, "Comparison of two railgun power supply architectures to quantify the energy dissipated after the projectile leaves the railgun," M.S. thesis, Dept. Elect. & Comp. Eng., Naval Postgraduate School, Monterey, CA, 2016.

[10] S. M. Lombardo, "Characterization of Anodized Titanium-based Novel Paradigm Supercapacitors: Impact of Salt Identity and Frequency on Dielectric Values, Power and Energy Densities," M.S. thesis, Dept. Mech. Eng., Naval Postgraduate School, Monterey, CA, 2017.

[11] J. Blau, "Directed energy weapons: power and energy requirements," 2014.

[12] "Panasonic develops new higher-capacity 18650 Li-Ion cells; application of silicon-based alloy in anode." *Green Car Congress,* pp. Sept 3, 2015, Dec 2009,

[13] S. Fromille and J. Phillips, "Superdielectric materials," *Materials*, vol. 7, 8197–8212, 2014. doi: 10.3390/ma7128197

[14] S. Fromille, "Novel concept for high dielectric constant composite electrolyte dielectrics," M.S. thesis, Dept. Mech. Eng., Naval Postgraduate School, Monterey, CA, 2013.

[15] N. L. Jenkins, "Optimal superdielectric material," M.S. thesis, Dept. Mech. Eng., Naval Postgraduate School, Monterey, CA, 2015.

[16] I. McNab and F. Beach, "Naval railguns," *Magnetics, IEEE Transactions On,* vol. 43, pp. 463–468, Jan. 2007.

[17] R. Natarajan, *Power System Capacitors.* Boca Raton, FL: Taylor & Francis, 2005.

[18] R. Marbury, *Power Capacitors.* McGraw-Hill Book Co., 1949.

[19] *PHYS208 Fundamentals of Physics II*. (9 March 1998). Available: "http://www.physics.udel.edu/~watson/phys208/parallel-plate.html".

[20] G. Feng, R. Qiao, J. Huang, B. Sumpter, and V. Meunier, "Computational modeling of carbon nanostructures for energy storage applications," presented at 10th IEEE International Conference on Nanotechnology Joint Symposium with Nano Korea, Seoul, Republic of Korea, 2010.

[21] J. W. Gandy, "Characterization of micron-scale nanotubular superdielectric materials," M.S. thesis, Dept. Mech. Eng., Naval Postgraduate School, Monterey, CA, 2015.

[22] F. J. Q. Cortes and J. Phillips, "Tube-superdielectric materials: electrostatic capacitors with energy density greater than 200 J·cm-3," *Materials,* vol. 8, 6208–6227, Sep 2015. doi: 10.3390/ma8095301

[23] J. Phillips, F. Quintero, and Suarez, "Toward a Universal Model of High Energy Density Capacitors," unpublished, 2017.

[24] N. Jenkins, C. Petty, and J. Phillips, "Investigation of fumed silica/aqueous NaCl superdielectric material," *Materials,* vol. 9, no. 2, p. 118, Feb 2016.

[25] (2009). Physics 51-electricity & magnetism: \Capacitors [Online]. Available: http://www.physics.sjsu.edu/becker/physics51/capacitors.htm.

[26] "Murata Supercapacitor Technical Note." *Murata*. (n.d.). No. C2M1CXS-053L. [Online].Available: http://www.murata.com/~/media/webrenewal/products/capacitor/edlc/techguide/electrical/c2m1cxs-053.ashx. Accessed May 5, 2017.

[27] Celgard ® PP1615 Technical Data Sheet, product information.

THIS PAGE INTENTIONALLY LEFT BLANK

INITIAL DISTRIBUTION LIST

1. Defense Technical Information Center
   Ft. Belvoir, Virginia

2. Dudley Knox Library
   Naval Postgraduate School
   Monterey, California